



**HAL**  
open science

## **A compositional breakage equation for wheat milling**

S.P. Galindez-Najera, P. Choomjaihan, Cecile Barron, Valerie Lullien-Pellerin,  
G.M. Campbell

► **To cite this version:**

S.P. Galindez-Najera, P. Choomjaihan, Cecile Barron, Valerie Lullien-Pellerin, G.M. Campbell. A compositional breakage equation for wheat milling. *Journal of Food Engineering*, 2016, 182, pp.46-64. 10.1016/j.jfoodeng.2016.03.001 . hal-01837421

**HAL Id: hal-01837421**

**<https://hal.science/hal-01837421>**

Submitted on 28 May 2020

**HAL** is a multi-disciplinary open access archive for the deposit and dissemination of scientific research documents, whether they are published or not. The documents may come from teaching and research institutions in France or abroad, or from public or private research centers.

L'archive ouverte pluridisciplinaire **HAL**, est destinée au dépôt et à la diffusion de documents scientifiques de niveau recherche, publiés ou non, émanant des établissements d'enseignement et de recherche français ou étrangers, des laboratoires publics ou privés.

# Accepted Manuscript

A compositional breakage equation for wheat milling

S.P. Galindez-Najera, P. Choomjaihan, C. Barron, V. Lullien-Pellerin, G.M. Campbell



PII: S0260-8774(16)30060-7

DOI: [10.1016/j.jfoodeng.2016.03.001](https://doi.org/10.1016/j.jfoodeng.2016.03.001)

Reference: JFOE 8499

To appear in: *Journal of Food Engineering*

Received Date: 16 November 2015

Revised Date: 1 March 2016

Accepted Date: 2 March 2016

Please cite this article as: Galindez-Najera, S., Choomjaihan, P, Barron, C, Lullien-Pellerin, V, Campbell, G., A compositional breakage equation for wheat milling, *Journal of Food Engineering* (2016), doi: 10.1016/j.jfoodeng.2016.03.001.

This is a PDF file of an unedited manuscript that has been accepted for publication. As a service to our customers we are providing this early version of the manuscript. The manuscript will undergo copyediting, typesetting, and review of the resulting proof before it is published in its final form. Please note that during the production process errors may be discovered which could affect the content, and all legal disclaimers that apply to the journal pertain.

Comment citer ce document :

Galindez-Najera, S., Choomjaihan, P., Barron, C., Lullien-Pellerin, V., Campbell, G. (2016). A compositional breakage equation for wheat milling. *Journal of Food Engineering*, 182, 46–64.  
DOI : 10.1016/j.jfoodeng.2016.03.001

## A compositional breakage equation for wheat milling

Galindez-Najera SP<sup>1</sup>, Choomjaihan P<sup>2</sup>, Barron C<sup>3</sup>, Lullien-Pellerin V<sup>3</sup> and Campbell GM<sup>1,4\*</sup>

1. Satake Centre for Grain Process Engineering, School of Chemical Engineering and Analytical Science, The University of Manchester, Oxford Rd, Manchester, M13 9PL, UK

2. Curriculum of Agricultural Engineering, Department of Mechanical Engineering, Faculty of Engineering, King Mongkut's Institute of Technology Ladkrabang, Bangkok, 10520, Thailand

3. UMR 1208 Ingénierie des Agropolymères et Technologies Emergentes, INRA, UMII, Cirad, Montpellier Supagro 2, Place P. Viala, bâtiment 31, 34060 Montpellier Cedex 2, France

4. Current address: School of Applied Sciences, University of Huddersfield, Queensgate, Huddersfield, HD1 3DH, UK

\* corresponding author: g.campbell@hud.ac.uk

### Abstract

The compositional breakage equation is derived, in which the distributions of botanical components following milling of wheat are defined in terms of compositional breakage functions and concentration functions. The forms of the underlying functions are determined using experimental data for Outer Pericarp, Intermediate Layer, Aleurone and Starchy Endosperm generated from spectroscopic analysis of milled fractions of a hard and a soft wheat milled under Sharp-to-Sharp (S-S) and Dull-to-Dull (D-D) dispositions. For the hard Mallacca wheat, the Outer Pericarp, Intermediate Layer and Aleurone compositions mostly varied with particle size in similar ways, consistent with these layers fusing together as “bran” and breaking together, although with possibly a subtle difference around the production of very fine particles under D-D milling. By contrast, for the soft Consort wheat, Outer Pericarp, Intermediate Layer and Aleurone were distributed in broken particles very differently, particularly under D-D milling, suggesting a different breakage mechanism associated with differences in the mechanical properties and adhesion of the bran layers. These new insights into the nature of wheat breakage and the contributions of the component tissues could have implications for wheat breeding and flour mill operation.

### Keywords

flour milling; composition; pericarp; aleurone; endosperm; breakage function

## 36 Introduction

37 In the 1950s Broadbent and Callcott introduced breakage matrices to relate input and output  
38 particle size distributions during grinding operations (Broadbent and Callcott, 1956a, 1956b,  
39 1957). They used square matrices in which the input and output particle size distributions  
40 covered the same size ranges, and applied this approach to model coal grinding. Campbell  
41 and Webb (2001) applied the breakage matrix approach to roller milling of wheat, extending  
42 the approach to use non-square matrices covering different size ranges for the input and  
43 output particle size distributions, thus improving the applicability and accuracy of the  
44 approach.

45 A complete understanding of milling requires the ability to predict the size distribution of  
46 broken particles and also the composition of particles of different sizes. Fistes and Tanovic  
47 (2006) demonstrated that compositional breakage matrices could also be constructed that,  
48 combined with breakage matrices for predicting output particle size, allowed the composition  
49 of those output particles also to be predicted. They also employed roller milling of wheat as  
50 the system with which to demonstrate the value of predictions for composition as well as  
51 size; the key feature of roller milling of wheat is that the bran tends to stay as large particles  
52 and the endosperm as small particles, hence facilitating separation of bran and endosperm by  
53 sifting.

54 Subsequent work by Campbell and co-workers focussed on the continuous form of the  
55 breakage equation and of breakage functions, rather than the discrete forms that underpin the  
56 construction of breakage matrices; continuous functions are more generally applicable and  
57 more readily interpretable, thus yielding greater predictive power and greater mechanistic  
58 insights regarding wheat breakage. This body of work has allowed the effects on the output  
59 particle size distribution of roll gap, roll disposition, wheat kernel hardness, moisture content  
60 and shape to be quantified (Campbell and Webb, 2001; Campbell *et al.*, 2001, 2007, 2012;  
61 Fang and Campbell, 2003a,b; Fuh *et al.*, 2014). The objectives of the current work are to  
62 demonstrate that continuous breakage functions can also be defined in relation to particle  
63 composition, for use alongside breakage functions that predict particle size distribution, and  
64 to generate experimental data to begin to identify the form and significance of those functions  
65 and the new insights they reveal. The current work thus represents the continuous equivalent  
66 of the discrete compositional breakage matrices introduced by Fistes and Tanovic (2006).

67

68 **Theory**

69 The breakage equation for roller milling of wheat in its cumulative form is

$$70 \quad P_2(x) = \int_0^{\infty} B(x, D) \rho_1(D) dD \quad (1)$$

71 where  $D$  is the input particle size,  $x$  is the output particle size,  $P_2(x)$  is the proportion by mass  
 72 of output material smaller than size  $x$ ,  $B(x, D)$  is the breakage function and  $\rho_1(D)$  is the  
 73 probability density function describing the input particle size distribution (Campbell *et al.*,  
 74 2007). The logic of the breakage equation is that the total mass of particles smaller than a  
 75 given size  $x$  arises from contributions from all the inlet particles. The contribution from inlet  
 76 particles initially of size  $D$  depends on how many of those particles there are (which is  
 77 quantified by  $\rho_1(D)$ ) and on how those particles break (which is quantified by the breakage  
 78 function,  $B(x, D)$ ). The total mass is found by integrating all of these contributions over the  
 79 range of inlet particle sizes.

80 Applying equivalent logic, the composition of particles can also be described and related to  
 81 the particle size distribution. Choomjaihan (2009) derives the relationships by proposing that  
 82 the entire wheat kernel, and its milled fractions, can be considered to be made up of four  
 83 main components: Pericarp (including testa and nucellar tissue), Aleurone, Starchy  
 84 Endosperm and Germ. The sum of the proportions of these four components is unity:

$$85 \quad X_{pe} + X_{al} + X_{en} + X_{ge} = 1 \quad (2)$$

86 where  $X_{pe}$  is the proportion of the whole wheat that is Pericarp,  $X_{al}$  is the proportion of the  
 87 whole wheat that is Aleurone,  $X_{en}$  is the proportion of the whole wheat that is Endosperm,  
 88 and  $X_{ge}$  is the proportion of the whole wheat that is Germ. Typically  $X_{pe}$  would be about 8%,  
 89  $X_{al}$  about 7%,  $X_{en}$  about 82% and  $X_{ge}$  about 3% (Pomeranz, 1988).

90 On breakage, particles are formed that individually may contain Pericarp, Aleurone,  
 91 Endosperm and Germ in different proportions. In general, the particles in a size range, say  
 92 from 100-200  $\mu\text{m}$ , will have a proportion of each component that will be different from  
 93 particles in a different size range, say 2000-2100  $\mu\text{m}$ ; the smaller particles are likely to  
 94 contain more Endosperm material, the larger particles more bran material (*i.e.* Pericarp and  
 95 Aleurone).

96 Consider the total proportion of outlet particles smaller than size  $x$ , given by  $P_2(x)$ . These  
 97 particles, as a whole, are made up of a proportion of Pericarp, a proportion of Aleurone, a  
 98 proportion of Endosperm, and a proportion of Germ. The total amount of particles smaller  
 99 than size  $x$  is made up of the total Pericarp that is in particles smaller than size  $x$ , plus the  
 100 total Aleurone that is in particles smaller than  $x$ , plus the total Endosperm that is in particles  
 101 smaller than  $x$ , plus the total Germ that is in particles smaller than  $x$ . Mathematically:

$$\begin{aligned}
 P_2(x) &= \frac{\text{total mass of particles smaller than } x}{\text{total mass}} \\
 &= \sum_i X_i \cdot Y_i(x) \\
 &= X_{pe} \cdot Y_{pe}(x) + X_{al} \cdot Y_{al}(x) + X_{en} \cdot Y_{en}(x) + X_{ge} \cdot Y_{ge}(x)
 \end{aligned} \tag{3}$$

103 where  $Y_{pe}(x)$  is the proportion (by mass) of the total Pericarp that is in particles smaller than  
 104  $x$ , and so on for  $Y_{al}(x)$ ,  $Y_{en}(x)$  and  $Y_{ge}(x)$ . Figure 1 illustrates how the distributions of the four  
 105 components sum to give the total particle size distribution. Figure 2 illustrates the  
 106 distributions in their non-cumulative forms. (Note that in Figures 1 and 2, the proportions of  
 107 the four components are unrealistic, having been set at 20%, 10%, 67% and 3% arbitrarily,  
 108 just to separate out the lines in order to illustrate the point. The shapes of the curves are also  
 109 arbitrary, contrived to show Endosperm predominantly breaking into small particles, Pericarp  
 110 and Aleurone staying in larger particles, and Germ forming a narrow peak within the mid-  
 111 range particles.)

112 For example, consider the more realistic situation that in the whole wheat,  $X_{pe} = 0.08$ ,  $X_{al} =$   
 113  $0.07$ ,  $X_{en} = 0.82$ ,  $X_{ge} = 0.03$ . The wheat is milled, forming particles ranging in size from 0 up  
 114 to 4000  $\mu\text{m}$ , with most of the particles at the smaller end of the range. Consider just those  
 115 particles that are smaller than 500  $\mu\text{m}$ . Imagine that 40% of the total Pericarp has ended up  
 116 in those particles; the other 60% is in particles that have remained larger than 500  $\mu\text{m}$ .  
 117 However, the Aleurone has not broken so readily, so only 30% of the total Aleurone has  
 118 ended up in the particles smaller than 500  $\mu\text{m}$ ; 70% of the Aleurone has stayed in the larger  
 119 particles. The Endosperm has broken easily; 80% of the Endosperm is now in small  
 120 particles, with only 20% in large particles. Meanwhile, the Germ is evenly split; half of the  
 121 Germ material is in particles that are smaller than 500  $\mu\text{m}$ . Thus:

$$122 \quad Y_{pe}(500) = 0.40, Y_{al}(500) = 0.30, Y_{en}(500) = 0.80, Y_{ge}(500) = 0.50$$

123 Then, the total proportion of particles smaller than 500  $\mu\text{m}$  is given by

$$\begin{aligned}
 P_2(x) &= 0.08 \times 0.4 + 0.07 \times 0.3 + 0.82 \times 0.8 + 0.03 \times 0.5 \\
 124 \quad &= 0.032 + 0.021 + 0.656 + 0.015 \\
 &= 0.724
 \end{aligned}$$

125 *i.e.* 72.4% of particles are smaller than 500  $\mu\text{m}$ . Taking these particles as a whole, they are  
 126 made up of  $0.032/0.724=4.4\%$  Pericarp, 2.9% Aleurone, 90.6% Endosperm and 2.1% Germ,  
 127 *i.e.* they are enriched in Endosperm, and depleted in the other components, compared with the  
 128 material as a whole.

129 This is a contrived example, to illustrate the mathematics, but it reflects the known behaviour  
 130 of wheat during breakage, that bran material (Pericarp and Aleurone) tends to stay in large  
 131 particles, while endosperm shatters more readily into smaller particles. Thus, separation on  
 132 the basis of size using repeated milling and sifting allows separation of the bran from  
 133 endosperm to produce relatively pure white flour. As in the contrived example here, one  
 134 would expect smaller particles to be enriched in endosperm material, compared with the  
 135 endosperm content of the whole wheat.

136 Now, taking the Pericarp as an example, the Pericarp concentration in this group of particles,  
 137  $Y_{pe}^*(x)$ , is given by the total amount of Pericarp in particles smaller than  $x$ , divided by the  
 138 total amount of particles smaller than  $x$ . The latter is the sum of the individual components,  
 139 hence:

$$\begin{aligned}
 Y_{pe}^*(x) &= \frac{\text{mass of component } i \text{ in particles smaller than } x}{\text{total mass in particles smaller than } x} \\
 140 \quad &= \frac{X_{pe} \cdot Y_{pe}(x)}{P_2(x)} \tag{4} \\
 &= \frac{X_{pe} \cdot Y_{pe}(x)}{X_{pe} \cdot Y_{pe}(x) + X_{al} \cdot Y_{al}(x) + X_{en} \cdot Y_{en}(x) + X_{ge} \cdot Y_{ge}(x)}
 \end{aligned}$$

$$\begin{aligned}
 141 \quad Pe'(x) &= \frac{Pe_{tot} \times Pe(x)}{P_2(x)} \tag{5} \\
 &= \frac{Pe_{tot} \times Pe(x)}{Pe_{tot} \times Pe(x) + Al_{tot} \times Al(x) + En_{tot} \times En(x) + Ge_{tot} \times Ge(x)}
 \end{aligned}$$

142 and similarly for the concentrations of the other components, defined as  $Y_{al}^*(x)$ ,  $Y_{en}^*(x)$  and  
 143  $Y_{ge}^*(x)$ . Similarly to  $X_i$ , the sum of all  $Y_i^*$  concentrations must be unity:

$$144 \quad \sum_i Y_i^*(x) = Y_{pe}^*(x) + Y_{al}^*(x) + Y_{en}^*(x) + Y_{ge}^*(x) = 1 \tag{6}$$

145 Referring to Figure 1,  $X_{pe}(x)$  is defined by the point A divided by the point C (the amount of  
 146 Pericarp in particles smaller than  $x$  divided by the total amount of Pericarp), while  $Y_{pe}^*(x)$  is  
 147 defined by the point A divided by the point B (the amount of Pericarp in particles smaller  
 148 than  $x$  divided by the total amount of particles smaller than  $x$ , *i.e.* the average concentration of  
 149 Pericarp in particles smaller than  $x$ ). Note that this is the average concentration across all of  
 150 the particles smaller than  $x$ . The concentration of Pericarp in particles of size  $x$  will be  
 151 different from this average. We turn our attention to this now.

152 The preceding paragraphs have focussed on cumulative probability density functions. The  
 153 probability density function for component  $i$  in its non-cumulative form,  $\rho_i(x)$ , is defined as:

$$154 \quad \rho_i(x) = \frac{d}{dx} Y_i(x) \quad (7)$$

155 The quantity  $\rho_i(x)dx$  is the proportion of the total component  $i$  that is in particles of size  $x$ ,  
 156  $x+dx$ . Multiplying this by the total proportion of component  $i$  in the material as a whole gives  
 157 the total of the material as a whole that is component  $i$  and that is in the size range  $x, x+dx$ .  
 158 This is equal to the proportion of total material in the size range  $x, x+dx$ , multiplied by the  
 159 component  $i$  concentration of that material. Figure 2 illustrates for Pericarp the two ways of  
 160 defining this quantity of material, based on the particle size distribution and composition, or  
 161 on the Pericarp total and distribution, showing that they are equivalent. This equivalence is  
 162 expressed mathematically as:

$$163 \quad X_i \rho_i(x) dx = \rho_2(x) y_i(x) dx \quad (8)$$

164 where  $\rho_2(x)$  is the probability density function describing the outlet particle size distribution,  
 165 and  $y_i(x)$  is the concentration of component  $i$  in particles of size  $x$ . Thus the amount of  
 166 material defined by the brown area in Figure 2 is the value of the probability density function  
 167 for Pericarp at that point,  $\rho_{pe}(x)$ , multiplied by  $dx$  and by the total proportion of Pericarp,  $X_{pe}$ .  
 168 This is equal to the total amount of material in the range  $x+dx$  multiplied by the concentration  
 169 of Pericarp in that total,  $y_{pe}(x)$ .

170 Similarly,  $y_{al}(x)$  is the concentration of Aleurone material,  $y_{en}(x)$  is the concentration of  
 171 Endosperm material and  $y_{ge}(x)$  is the concentration of Germ material in particles of size  $x$ .  
 172 Clearly

$$173 \quad \sum_i y_i(x) = y_{pe}(x) + y_{al}(x) + y_{en}(x) + y_{ge}(x) = 1 \quad (9)$$



174 and

$$175 \quad \sum_i X_i \rho_i(x) = \rho_2(x) \sum_i y_i(x) = \rho_2(x) \quad (10)$$

176 The breakage equation is given by Eqn. (1). If  $D$  is essentially monodispersed (little variation  
177 in wheat kernel size), then the breakage is described by  $P_2(x) = B(x,D)$  or, more generally, by  
178  $B(x,G/D)$  – the proportion of particles smaller than  $x$  arising from breakage of wheat at a  
179 given milling ratio  $G/D$ , where  $G$  is the roll gap. The functions  $y_i(x)$  similarly become  
180  $y_i(x,G/D)$ , the proportion of botanical component  $i$  in particles of size  $x$  resulting from milling  
181 wheat at a milling ratio  $G/D$ . If the  $y_i(x,G/D)$  are known, then both the size distribution of  
182 particles following breakage and their compositions can be predicted. Thus the  
183 compositional breakage equation is:

$$184 \quad \begin{aligned} P_2(x,G/D) &= \sum_i X_i \cdot Y_i(x,G/D) = \sum_i X_i \cdot \int_0^x \rho_i(x,G/D) \cdot dx \\ &= \sum_i \int_0^x \rho_2(x,G/D) \cdot y_i(x,G/D) \cdot dx \end{aligned} \quad (11)$$

185 and in its non-cumulative form:

$$186 \quad \begin{aligned} \rho_2(x,G/D) &= \sum_i X_i \cdot \rho_i(x,G/D) \\ &= \sum_i \rho_2(x,G/D) \cdot y_i(x,G/D) \end{aligned} \quad (12)$$

187 Equations 11 and 12 allow both the particle size distribution, and the composition of each  
188 size fraction, to be described by a single equation. This simplifies the problem to establishing  
189 “concentration functions” to describe  $y_{pe}(x,G/D)$ ,  $y_{al}(x,G/D)$ ,  $y_{en}(x,G/D)$  and  $y_{ge}(x,G/D)$ ,  
190 leading to “compositional breakage functions” that describe  $\rho_{pe}(x,G/D)$ ,  $\rho_{al}(x,G/D)$ ,  
191  $\rho_{en}(x,G/D)$  and  $\rho_{ge}(x,G/D)$ . This could be done by milling wheat at different roll gaps, sifting  
192 it into difference size fractions, and measuring the compositions of those size fractions, *i.e.*  
193 the relative proportions of Pericarp, Aleurone, Endosperm and Germ in each fraction.  
194 Knowing how these relative compositions change, curves could then in principle be fitted to  
195 describe these changes as functions of  $x$  and  $G/D$ . Ultimately, of course, with a very large  
196 experimental programme, these compositional breakage functions could be extended to  
197 include hardness, as Campbell *et al.* (2007) did for the size-based breakage function. These  
198 ambitions were beyond the scope of the current work.

199 Equations 11 and 12 represent the continuous equivalent of the discrete compositional  
 200 breakage matrices introduced by Fistes and Tanovic (2006). The equations presented here are  
 201 continuous functions that are more generally applicable and more readily interpretable.

202

### 203 **Identifying the form of compositional breakage functions**

204 Having derived the compositional breakage equation above, the first objective of the current  
 205 work, the second objective is to begin to understand the form of the compositional breakage  
 206 functions by generating experimental data. In principle this is as simple as measuring the  
 207 concentrations of Pericarp, Aleurone, Endosperm and Germ in size fractions following  
 208 milling, and fitting functions to describe the variation. However, there are two difficulties  
 209 with this. Firstly, these concentration functions are not probability density functions and  
 210 hence do not have the well defined constraints of probability density functions that allow easy  
 211 fitting. Secondly, measuring the proportions of these materials in milled wheat samples is not  
 212 straightforward.

213 Taking the first of these issues, Eqn. (8) can be rearranged to give

$$214 \quad y_i(x) = \frac{X_i \rho_i(x)}{\rho_2(x)} \quad (13)$$

215 where

$$216 \quad \rho_2(x) = \frac{d}{dx} P_2(x) \quad (14)$$

217 and  $\rho_i(x)$  is similarly the derivative of  $Y_i(x)$  as defined in Eqn. 7. Campbell *et al.* (2012)  
 218 introduced the Double Normalised Kumaraswamy Breakage Function (DNKBF) as a flexible  
 219 probability density function well suited to describing the particle size distributions arising  
 220 from roller milling of wheat, and having a cumulative form that is easy to fit and is then  
 221 differentiable. Assuming this function has the flexibility to describe  $Y_i(x)$  as well, from  
 222 which  $\rho_i(x)$  could be obtained by differentiation, Eqn. 13 then allows  $y_i(x)$ , the concentration  
 223 of component  $i$  in particles of size  $x$ , to be calculated as the ratio of these two probability  
 224 density functions. This approach, involving fitting a cumulative probability density function  
 225 to the accumulated data, is likely to deal with inaccuracies in the experimental data more  
 226 effectively, and to yield more meaningful descriptions of the compositional breakage  
 227 functions, than attempting to fit the concentration data directly.

228 The second issue identified above is that of experimentally measuring the composition of  
229 milled fractions. In principle this can be done using suitable biochemical markers specific for  
230 each tissue type (Peyron *et al.*, 2002; Barron *et al.*, 2007; Barron and Rouau, 2008; Hemery *et*  
231 *al.*, 2009; Barron *et al.*, 2011). However, Barron (2011) predicted the relative tissue  
232 proportion in wheat mill streams by FTIR spectroscopy and PLS analysis. In that study,  
233 Aleurone Layer, Intermediate Layer (composed of three layers: hyaline layer, testa and inner  
234 pericarp (Barron *et al.*, 2007; Barron, 2011), Outer Pericarp and Starchy Endosperm were  
235 isolated as in previous works from the same author from various common wheat cultivars.  
236 (Germ constitutes about 3% of the grain; its omission adds an error of a magnitude that is  
237 within the analytical error of the method.) Different milled streams arising from debranning,  
238 conventional milling and bran fractionation were produced from two French wheat varieties.  
239 The spectra of botanical tissues and milled fractions were collected with a FTIR coupled with  
240 an ATR device. The biochemical markers technique studied by the same author was used as  
241 the reference method (Barron *et al.*, 2007; Hemery *et al.*, 2009; Barron *et al.*, 2011). PLS  
242 models were developed to predict the proportion of the botanical tissues in the milled  
243 streams. The predictions obtained were good despite the complex natures and compositions  
244 of botanical tissues. These models were used in the current work to quantify the  
245 compositions of milled fractions in order to fit compositional breakage functions.

246

## 247 **Materials and Methods**

248 In order to demonstrate the compositional breakage equation approach, in the current work a  
249 hard UK wheat, Mallacca (average hardness = 52.5, average mass = 47.6 mg, average  
250 diameter = 3.26 mm after conditioning, as measured by the Single Kernel Characterisation  
251 System Model 4100 (Perten Instruments, Sweden)) and a UK soft wheat, Consort (SKCS  
252 hardness = 33.9, average mass = 34.7 mg, average diameter = 2.89 mm after conditioning)  
253 were conditioned to 16% moisture (wet basis). 100 g samples were milled on the Satake  
254 STR100 mill (Satake Corporation, Hiroshima, Japan) at a roll gap of 0.5 mm under Sharp-to-  
255 Sharp (S-S) and Dull-to-Dull (D-D) dispositions, and separated by sifting into eight fractions  
256 using sieves of size 2000, 1700, 1400, 1180, 850, 500 and 212  $\mu\text{m}$ , using equipment and  
257 methods described elsewhere (Campbell *et al.*, 2007). The milled fractions were analysed  
258 using Barron's spectroscopy-based models, in order to estimate the proportions of Outer  
259 Pericarp, Intermediate Layer, Aleurone and Starchy Endosperm in each fraction. In total 34

260 samples were analyzed: two wheat types  $\times$  two dispositions  $\times$  one roll gap  $\times$  eight fractions =  
261 32, plus the two whole wheats = 34. This work is presented more fully in Galindez-Najera  
262 (2014). No replication was undertaken due to practical limitations; within the constraints of  
263 the work, we preferred to generate data from contrasting wheats and milling conditions, to  
264 serve the purposes of illustrating the approach and allowing tentative new insights.

265 The protocol for spectroscopic analysis of the samples was based on the method described by  
266 Barron (2011): milled fractions were first ground in liquid nitrogen with a Spex CertiPrep  
267 6750 laboratory impact grinder to have a homogenous size. Spectra were recorded in the MIR  
268 region using a Nicolet Nexus 6700 (ThermoScientific, Courtaboeuf, France) spectrometer  
269 equipped with an ATR Smart DuraSampleIR accessory (ThermoScientific, U.K.) and a  
270 Mercury Cadmium-Telluride-High D detector. Spectra were recorded between 800 and 4000  
271  $\text{cm}^{-1}$ , with samples pressed onto the diamond ATR area. Interferograms (128) were collected  
272 at 4  $\text{cm}^{-1}$  resolution and co-added before Fourier transformation. For each sample five  
273 spectra were collected. An air-background scan was recorded every three spectra. Partial  
274 Least Square (PLS) quantification was applied using models developed by Barron (2011).  
275 Similar spectral pre-treatments were then applied to predict each tissue proportion. Outer  
276 Pericarp, Intermediate Layer (including inner pericarp), Aleurone and Starchy Endosperm  
277 were predicted in each milled fraction, and the results interpreted through the compositional  
278 breakage equation.

279 A number of cautions are emphasised at this point. Firstly, we acknowledge that the  
280 correlations used in the model were based on French wheats, such that the absolute results  
281 generated for these UK samples are unlikely to be accurate. However, the relative values are  
282 likely to be sufficiently meaningful to allow the approach here to be demonstrated and to  
283 yield valid insights. Secondly, the models do not allow quantification of the Germ, and they  
284 distinguish between the Outer Pericarp and the Intermediate Layer. The information they  
285 provide is therefore not quite in the form of the derivations above, in particular not intending  
286 to provide mutually exclusive proportions of components that sum to unity. The values for  
287 Outer Pericarp, for example, should be considered to indicate how the Outer Pericarp  
288 concentration varies with particle size, but the corresponding variations of Intermediate  
289 Layer, Aleurone and Endosperm are not expected to sum to one. Thus the data can be used in  
290 conjunction with Eqn. 12 to find the form of the compositional breakage functions but not  
291 their absolute values, and could not be used at this stage to define completely Eqn. 11, the

292 compositional breakage equation. We also acknowledge that the individual trials were not  
293 replicated.

294

## 295 **Results and Discussion**

296 Table 1 shows the proportion of material on each sieve size following milling under S-S or  
297 D-D, and the percentages of Outer Pericarp, Intermediate Layer, Aleurone and Starchy  
298 Endosperm in each fraction as predicted by Barron's model, along with the predictions for  
299 each component in whole wheat samples. Note that the independent raw data for each  
300 component did not sum to unity, due to inherent errors in the predictions and in their  
301 application to UK wheats; on average the total material was overestimated by 8.3% for the  
302 Mallacca samples and 4.9% for Consort, possibly suggesting that the French wheats used to  
303 generate the models were more similar to the soft Consort wheat, although the discrepancy is  
304 within the accuracy of the method. The data reported in Table 1 have been normalised to  
305 unity, as a reasonable approximation to the composition of particles in each size range, and to  
306 fit the assumptions underlying the formulation of the compositional breakage equation.

307 The total percentage of each component in the whole Mallacca wheat was  $X_{pe} = 8.3\%$ ,  $X_{Inlay} =$   
308  $1.2\%$ ,  $X_{al} = 6.0\%$  and  $X_{en} = 84.4\%$ ; and in the whole Consort wheat was  $X_{pe} = 2.3\%$ ,  $X_{Inlay} =$   
309  $2.9\%$ ,  $X_{al} = 5.8\%$  and  $X_{en} = 88.9\%$ . Multiplying the amount of material on each sieve by the  
310 concentration of a given component, and summing these, allows the cumulative  
311 compositional distributions,  $Y_{pe}(x)$ ,  $Y_{al}(x)$ ,  $Y_{en}(x)$  and  $Y_{Inlay}(x)$  (the proportion by mass of the  
312 total botanical component that is in particles smaller than  $x$ ) to be calculated.

313 The total is reported as the average for each component in Table 1, for each wheat type under  
314 each milling disposition. Ideally, these averages would be the same under both dispositions,  
315 and identical with the predicted compositions of the whole grains. Inspection of Table 1  
316 shows that there are some significant discrepancies, which underline again the inherent errors  
317 in the prediction method and in its application to UK wheats. Nevertheless, the data allow  
318 the compositional breakage function approach to be demonstrated, with appropriate caution,  
319 and using the averages rather than the data for whole wheat in order to ensure internal  
320 consistency in the analysis. The justification for this is that the average values are averaged  
321 from eight measurements, compared with just one for the whole wheat samples, and that in  
322 any case the PLS models were developed for milled stocks rather than for whole wheats

323 (Barron, 2011), so the results for the milled fractions might be expected to be more accurate  
324 than those for the whole wheats.

325 Figure 3 shows the cumulative distributions for the particle size distribution and for the four  
326 component distributions, for the Mallacca wheat milled under a Sharp-to-Sharp disposition.  
327 Figure 4 presents the experimental data and the fitted size distributions in their non-  
328 cumulative forms. Table 2 reports the fitted Double Normalised Kumaraswamy Breakage  
329 Function parameters. In order to fit the DNKBF, the  $x$ -axis was normalised by dividing  
330 particle size by 4000  $\mu\text{m}$ , in order to yield Kumaraswamy shape parameters consistent with  
331 previously reported work, although the current work only used 2000  $\mu\text{m}$  for its largest sieve,  
332 so the data beyond this size is not available. The DNKBF in its cumulative form is  
333 (Campbell *et al.*, 2012)

$$334 \quad P_2(z) = \underbrace{\alpha \left(1 - (1 - z^{m_1})^{n_1}\right)}_{\text{Type 1 Breakage}} + \underbrace{(1 - \alpha) \left(1 - (1 - z^{m_2})^{n_2}\right)}_{\text{Type 2 Breakage}} \quad (15)$$

335 where  $z$  is the normalized size,  $P(z)$  is the percentage smaller than  $z$ ,  $\alpha$  is the proportion of the  
336 distribution that can be described as Type 1 breakage, and  $m_1$  and  $n_1$  are parameters  
337 corresponding to Type 1 breakage. The quantity  $(1 - \alpha)$  gives the proportion of Type 2  
338 breakage, while  $m_2$  and  $n_2$  are the parameters that describe the form of Type 2 breakage.  
339 Differentiating Eqn. 14 gives the non-cumulative form of the DNKBF:

$$340 \quad p_2(z) = \underbrace{\alpha \left(m_1 n_1 z^{m_1 - 1} (1 - z^{m_1})^{n_1}\right)}_{\text{Type 1 Breakage}} + \underbrace{(1 - \alpha) \left(m_2 n_2 z^{m_2 - 1} (1 - z^{m_2})^{n_2}\right)}_{\text{Type 2 Breakage}} \quad (16)$$

341 Considering the particle size distributions in Figure 3(a) and Figure 4(a), the DNKBF  
342 describes the data well, yielding values of  $\alpha = 0.36$ ,  $m_1 = 5.54$ ,  $n_1 = 178.10$ ,  $m_2 = 1.08$  and  $n_2$   
343  $= 3.44$ ; these values are broadly consistent with previous work for a wheat of hardness  
344 around 50 milled under S-S (Campbell *et al.*, 2012).

345 Figures 3(a) and 4(a) also show the Type 1 and Type 2 functions that combine to give the  
346 DNKBF. The values of  $m_1$  and  $n_1$  describe a narrow peak of mid-range particles, while those  
347 for  $m_2$  and  $n_2$  describe a broad distribution of mostly small particles but extending to include  
348 the very large particles. Galindez-Najera and Campbell (2014) described a mechanism for  
349 Type 2 breakage that explains the co-production of the very large bran particles and the small  
350 Endosperm particles, and hence why they are described by the same Type 2 breakage  
351 function.

352 Considering now the cumulative distribution shown for the Outer Pericarp material in Figure  
353 3(b) and the non-cumulative form in Figure 4(b), again the DNKBF describes the data well.  
354 Comparing Figures 4(a) and 4(b), it appears that the Outer Pericarp is noticeably concentrated  
355 in the mid-range particles. The DNKBF shape parameters are  $m_1 = 4.05$ ,  $n_1 = 53.9$ ,  $m_2 = 0.38$   
356 and  $n_2 = 0.91$ , with the proportion of Type 1 breakage,  $\alpha = 0.733$ . The decrease in the Type 1  
357 parameters has tended to make the Type 1 component of the distribution more narrow, while  
358 the proportion of Type 1,  $\alpha$ , has increased to 0.733. Thus, Outer Pericarp is predominantly  
359 found in the mid-range Type 1 particles resulting from breakage. This is a new insight into  
360 wheat breakage.

361 The Type 2 parameters have both decreased to well below 1, giving a very steep peak for the  
362 very small particles, matching the experimental data at that point. This suggests that there is  
363 a significant amount of Outer Pericarp in the very small particles. This can be understood as  
364 Pericarp “dust” that is produced during breakage. Although bran material (Pericarp and  
365 Aleurone) tends to stay as large particles during roller milling, inevitably some small particles  
366 of bran (Outer Pericarp or beeswing) are produced, and this is evident here in the  
367 experimental data and in the modelling of it. Again, this is a new insight that is consistent  
368 with the accepted physical understanding of the nature of wheat breakage, but here has for the  
369 first time been identified and described quantitatively. It is proposed cautiously at this point,  
370 recognising that this work is for a single wheat and so far we have considered only a single  
371 component and only the S-S data. But it serves at this point to illustrate the nature of the  
372 compositional breakage function interpretation and the insights that can result.

373 Moving to consider the results for the Aleurone layer, Figures 3(d) and 4(d) show very  
374 similar results to those for Outer Pericarp; this makes sense, as the Pericarp and Aleurone  
375 tend to fuse during conditioning and break together (Hemery *et al.*, 2007). The fit is not quite  
376 as good as for the Outer Pericarp, despite the spectroscopic model being in general more  
377 accurate for Aleurone than for Outer Pericarp (Barron, 2011). Nevertheless, the same  
378 features are evident: a greater concentration of Aleurone material in mid-range Type 1  
379 particles, and a similar spike of very small particles of Aleurone-containing “dust”. The  
380 proportion of Type 1 in this case is lower at 0.557, while  $m_1 = 5.20$ ,  $n_1 = 100$ ,  $m_2 = 0.63$  and  
381  $n_2 = 2.13$ , all larger than the corresponding values for Outer Pericarp. Not too much should  
382 be read into the fine detail of these changes, beyond noting that in general the increases in the  
383 values of the Kumaraswamy shape parameters move the distribution slightly to the right.  
384 This may suggest the Aleurone is more prevalent in slightly larger particles following

385 breakage – possibly Outer Pericarp, being on the outside, is “knocked off” these larger  
 386 particles more easily than Aleurone, although a physical mechanism is not obvious and the  
 387 data does not support excessive speculation at this point. However the more general point  
 388 that the compositional variation of particles is very similar for both the Outer Pericarp and  
 389 Aleurone, and information from these two different components points to similar conclusions  
 390 regarding the nature of mid-range particles and the production of bran dust.

391 Figures 3(c) and 4(c) show the results for the Intermediate Layer. This data is predicted by  
 392 the spectroscopic model least accurately, such that there is significant scatter in the data, but  
 393 the results show a similar pattern to those for Outer Pericarp and Aleurone, adding  
 394 confidence that the features apparent in the graphs for these two components are genuine.

395 Moving to Figures 3(e) and 4(e), the Starchy Endosperm shows contrasting behaviour to the  
 396 Outer Pericarp and Aleurone, being more predominant in the smaller particles, but with the  
 397 fitted curves featuring a dip at the very smallest particles, consistent with these particles  
 398 containing significant amounts of bran dust and hence less endosperm. The proportion of  
 399 Type 1 is 0.293, with  $m_1 = 6.30$ ,  $n_1 = 343$ ,  $m_2 = 1.18$  and  $n_2 = 3.98$ . The increase of  $m_2$  to >1  
 400 introduces the hump at the lower end of the Type 2 curve. There is still a significant Type 1  
 401 bump in the middle of the distribution, indicating that there is a lot of Endosperm material in  
 402 these mid-range Type 1 particles. This is for the simple reason that there are a lot of these  
 403 Type 1 particles. We must remember that these distributions combine the particle size  
 404 distribution and the composition of those particles, such that the shapes of these curves is  
 405 dominated by the shape of the overall particle size distribution. The fit to the data is good,  
 406 but this data does not show clearly the concentrations of components in these particles. We  
 407 will focus on the concentrations in a moment, once we have considered results for the  
 408 Intermediate Layer.

409 As noted above, the concentration functions can be found by inserting the Double  
 410 Kumaraswamy Functions fitted to the particle size distribution and to the compositional  
 411 distributions into Eqn. 12. Once again this is illustrated in relation to Outer Pericarp:

$$\begin{aligned}
 y_i(x) &= \frac{X_i \rho_i(x)}{\rho_2(x)} \\
 &= \frac{X_i \left[ \alpha (m_1 n_1 z^{m_1-1} (1-z^{m_1})^{n_1}) + (1-\alpha) (m_2 n_2 z^{m_2-1} (1-(1-z^{m_2})^{n_2})) \right]_{i \text{ distribution}}}{\left[ \alpha (m_1 n_1 z^{m_1-1} (1-z^{m_1})^{n_1}) + (1-\alpha) (m_2 n_2 z^{m_2-1} (1-(1-z^{m_2})^{n_2})) \right]_{\text{particle size distribution}}}
 \end{aligned} \tag{17}$$



413 Figure 5 shows the concentration functions resulting from dividing the fitted DNKBF  
414 functions using Eqn. 17, for all four components, compared with the original experimental  
415 data for each component's concentration. The agreement is good, as one would hope as it is  
416 a circular relationship – the experimental data was used to generate the compositional  
417 breakage functions, so the reverse analysis (which is what the ratio of the composition and  
418 particle size DNKBFs is) would be expected more or less to recreate the experimental data.  
419 Figure 5 simply reassures that the analysis does indeed reveal genuine features, while  
420 allowing continuous functions to be formulated that could not readily be formulated from the  
421 raw compositional data.

422 A number of further observations can be drawn. Firstly, although dividing one wiggly  
423 function by another wiggly function gives an even more wiggly function for which not every  
424 wiggle is meaningful, the curves obtained do seem to agree with the trends in the  
425 experimental data. The curves and data beyond 2000  $\mu\text{m}$  ( $z = 0.5$ ) should be largely ignored,  
426 as there was only one data point covering this entire range. But below 2000  $\mu\text{m}$  ( $z = 0.5$ ), the  
427 concentration of Outer Pericarp as shown by the curve is high initially and drops suddenly,  
428 indicating fine Outer Pericarp dust present as very small particles; the experimental data also  
429 shows this. The concentration then increases to a peak for the mid-range particles and begins  
430 to decrease again, features that are again reflected in the experimental data.

431 The curves and experimental data for Aleurone show the same general pattern, albeit with  
432 more scatter. The curves and data for the Starchy Endosperm show an inverse trend with  
433 lower concentrations in the finest and the mid-range particles. The trend is less pronounced  
434 because the Endosperm necessarily dominates the composition of all the particles.  
435 Meanwhile the overall trend is downwards, consistent with the expectation that larger  
436 particles are less concentrated in Endosperm than smaller particles. The Intermediate Layer  
437 seems to show a slightly increasing trend of concentration with particle size.

438 A further observation is that the concentration functions are clearly very complex; it would be  
439 not be possible to define a simple function likely to be capable of describing variations in  
440 component concentration for a range of wheats milled under a range of conditions. The  
441 approach presented here, allowing the particle size distribution and the component  
442 distributions to be described by Double Kumaraswamy Functions, the ratios of which give  
443 the concentration functions, is a practical way to describe, quantify and interpret the effects of  
444 breakage on component distributions.

445 Figures 6 and 7 show the equivalent results for the samples milled under a Dull-to-Dull  
446 disposition. The fitted DNKBF parameters are again reported in Table 2. Although this is  
447 the same wheat, in other respects these results are independent of those discussed above; the  
448 size fractions were generated and analysed independently of those produced from milling  
449 under S-S. It is encouraging that many of the features seen in the S-S data also appear here:  
450 the higher concentrations of Outer Pericarp and Aleurone in mid-range Type 1 particles, and  
451 higher concentration of Endosperm in smaller particles. A notable difference is the absence  
452 of evidence of Outer Pericarp in the very fine dust, although there is still evidence of  
453 Aleurone material in this fine dust, and also of Intermediate Layer, while there is a high  
454 concentration of Outer Pericarp in the slightly larger small particles. This probably reflects  
455 limitations in this small set of experimental data, but could conceivably reflect differences in  
456 the nature of breakage under Dull-to-Dull compared with Sharp-to-Sharp milling. Galindez-  
457 Najera and Campbell (2014) describe differences in the scraping of bran particles formed  
458 from Dull-to-Dull milling compared with Sharp-to-Sharp. Based on this description, it is  
459 plausible that D-D gives less creation of bran dust in the first place, but yields more effective  
460 scraping of Endosperm from the inside of the large bran particles, this scraping generating  
461 Aleurone and Intermediate Layer material in the finest particles, but not getting as far as  
462 Outer Pericarp. More extensive work would be needed to identify conclusively patterns of  
463 breakage under different conditions, but the results from D-D milling support those from S-S  
464 in demonstrating the quantitative interpretation that the compositional breakage function  
465 approach can deliver.

466 Figure 8 presents the experimental data and the fitted size distributions in their non-  
467 cumulative forms for Consort wheat. The fitted DNKBF parameters are again reported in  
468 Table 2.

469 Considering the particle size distribution in Figure 8(a), the DNKBF describes the data well,  
470 yielding values of  $\alpha = 0.143$ ,  $m_1 = 8.21$ ,  $n_1 = 1527$ ,  $m_2 = 0.99$  and  $n_2 = 2.24$ ; these values are  
471 broadly consistent with previous work for a wheat of hardness around 30, milled under S-S  
472 (Campbell *et al.*, 2012).

473 Figure 8(a) also show the Type 1 and Type 2 functions that combine to give the DNKBF. As  
474 a reminder, the values of  $m_1$  and  $n_1$  describe a narrow peak of mid-range particles, while  
475 those for  $m_2$  and  $n_2$  describe a broad distribution of mostly small particles but extending to  
476 include the very large particles.

477 Considering now the cumulative distribution shown for the Outer Pericarp in Figure 8(b),  
478 again the DNKBF describes the data well. Comparing Figures 8(a) and 8(b), it appears that  
479 the Outer Pericarp material is clearly concentrated in the mid-range particles. The DNKBF  
480 shape parameters are  $m_1 = 4.02$ ,  $n_1 = 53.9$ ,  $m_2 = 0.75$  and  $n_2 = 0.63$ , with the proportion of  
481 Type 1 breakage,  $\alpha = 0.790$ . The decrease in the Type 1 parameters, in general, makes the  
482 Type 1 component of the distribution narrower, while the proportion of Type 1 has increased.  
483 Thus, Outer Pericarp is predominantly found in the mid-range Type 1 particles resulting from  
484 breakage. These results are similar to the findings for Mallacca wheat.

485 Similar to Mallacca wheat, the Type 2 parameters for Consort wheat have both decreased to  
486 below 1, but unlike Mallacca, a very small steep spike for the very small particles is observed  
487 for Consort, matching the experimental data at that point. This suggests a little amount of  
488 Outer Pericarp “dust” in the very small particles that is produced during breakage. Although  
489 bran material tends to stay as large particles during roller milling, inevitably some small  
490 particles of bran are produced. Although this new insight is not as evident as it is for  
491 Mallacca, there is still evident in both the experimental data and in the modelling for Consort.  
492 It is proposed cautiously at this point, recognising that this work is only for two wheat types  
493 and so far only a single Consort component and only the S-S data have been considered. But  
494 it serves at this point to illustrate the nature of the compositional breakage function  
495 interpretation and the insights that can result.

496 Regarding the results for the Aleurone layer, Figure 8(d) show a similar pattern to those for  
497 Outer Pericarp, although unlike Outer Pericarp for Mallacca wheat, there is not a steep peak  
498 for the very small particles (less dust production). The fit is once again not quite as good as  
499 for the Outer Pericarp, despite the spectroscopic model being in general more accurate for  
500 Aleurone than for Outer Pericarp (Barron, 2011). This may indicate that Aleurone breakage  
501 during milling is less well defined than Outer Pericarp breakage. Similar to Outer Pericarp, a  
502 greater concentration of Aleurone material in mid-range Type 1 particles is evident, along  
503 with very small particles of Aleurone-containing “dust”, although not showing a spike. The  
504 proportion of Type 1 in this case is lower at 0.36, while  $m_1 = 5.65$ ,  $n_1 = 100$ ,  $m_2 = 1.24$  and  $n_2$   
505  $= 2.25$ , all larger than the corresponding values for Outer Pericarp. In general the increase in  
506 the values of the Kumaraswamy shape parameters moves the distribution slightly to the right.  
507 This may suggest once again the Aleurone is more prevalent in slightly larger particles  
508 following breakage; possibly Outer Pericarp, being on the outside, is eliminated from these  
509 larger particles more easily than Aleurone, or, perhaps the production of Aleurone is coming

510 from inside, in other words, the Starchy Endosperm has been scraped off, allowing the action  
511 of the rolls to reach the Aleurone.

512 Figure 8(c) show the results for the Intermediate Layer. As noted earlier, this data is predicted  
513 by the spectroscopic model least accurately, such that there is significant scatter in the data.  
514 However, the Intermediate Layer shows an opposite behaviour with respect to Outer Pericarp  
515 and Aleurone; the presence of Intermediate Layer material is considerable higher in the dust  
516 but lower in the mid-range particles are pushed towards the larger mid-range particles. This  
517 insight is interesting because, while the Intermediate Layer might be expected to behave  
518 similarly to Aleurone and Outer Pericarp as part of the bran layers, the data suggest that the  
519 shearing effect applied to this soft wheat causes the Intermediate Layer to crumble quite  
520 easily into small particles, while the Outer Pericarp and Aleurone on either side remain  
521 relatively intact. If true, this is a remarkable new insight into the nature of soft wheat  
522 breakage.

523 Figure 8(e) show for the Starchy Endosperm contrasting behaviour to the Outer Pericarp and  
524 Aleurone, being more predominant in the smaller particles. The proportion of Type 1 is  
525 0.124, with  $m_1 = 6.74$ ,  $n_1 = 343$ ,  $m_2 = 0.951$  and  $n_2 = 2.29$ . Similar to Mallacca wheat, there is  
526 a significant Type 1 bump in the middle of the distribution, indicating that there is a lot of  
527 endosperm material in these mid-range Type 1 particles. Again, this is for the simple reason  
528 that there are a lot of these Type 1 particles.

529 Figure 9 shows the concentration functions resulting from dividing the fitted DNKB  
530 functions using Equation 17, for all four components, compared with the original  
531 experimental data for each component's concentration. Similar to Mallacca data, the  
532 experimental Consort data was used to generate the compositional breakage functions, so the  
533 reverse analysis more or less recreates the experimental data. Similar to Mallacca wheat  
534 results, Figure 9 reassures that the analysis does indeed reveal genuine features, while  
535 allowing continuous functions to be formulated that could not readily be formulated from the  
536 raw compositional data.

537 Figures 10 and 11 show the equivalent results for the Consort samples milled under a D-D  
538 disposition. The fitted DNKBF parameters are again reported in Table 2.

539 It is well established that milling a soft wheat under a D-D disposition gives a much broader  
540 particle size distribution than milling a hard wheat under S-S (Campbell et al., 2007, 2012),  
541 and the results in Figure 10 reflect this. In terms of the compositional data, once again these

542 data are independent from those considered above, and it is again encouraging that many of  
543 the features seen in the S-S data also appear here: the higher concentrations of Outer Pericarp  
544 and Aleurone in mid-range Type 1 particles, and higher concentration of Endosperm in  
545 smaller particles. A notable difference is the absence of Outer Pericarp in the very fine dust,  
546 although there is still evidence of Aleurone material in this fine dust. The Intermediate Layer  
547 shows a high concentration of dust in the very small particles, while in the slightly larger  
548 small particles there is higher concentration of the Intermediate Layer which then decreases  
549 in the mid-range and larger particles. It is observed that Aleurone and Intermediate layer are  
550 generating more dust than Outer Pericarp, which seems to show very little or no dust  
551 production under D-D milling. Under S-S milling, the production of Aleurone dust is less  
552 compared with D-D milling, although Outer Pericarp dust is higher and Intermediate Layer  
553 seems to be even more. All these features are in contrast to the harder Mallacca wheat, in  
554 which overall, the bran dust production is considerable higher under both dispositions  
555 compared with the soft Consort wheat, and particularly higher under D-D disposition.  
556 Consistent with the description presented by Galindez-Najera and Campbell (2014), the  
557 breakage mechanism observed here seems to suggest a more effective scraping of endosperm  
558 from the inside of the large bran particles, this scraping generating Aleurone and Intermediate  
559 Layer material in the finest particles, but not getting as far as Outer Pericarp.

560 Figure 12 collects the Outer Pericarp, Intermediate Layer and Aleurone distributions together  
561 on the same graph, for both wheats under both dispositions. Gathering together the data from  
562 all four conditions highlights certain consistent patterns and some distinctive differences that  
563 together give a degree of confidence that the apparent effects are genuine. Most striking is  
564 the contrast between the hard Mallacca wheat and the soft Consort wheat, which is more  
565 striking than the difference between the S-S and D-D dispositions. There are some intriguing  
566 and tantalising patterns within the compositional data for Mallacca, most notably the aleurone  
567 peak being shifted to the right compared with the Outer Pericarp peak (which is also evident  
568 for Consort under S-S), and the apparent production of Outer Pericarp/Intermediate  
569 Layer/Aleurone “dust” under S-S, but only Intermediate Layer/Aleurone dust, without Outer  
570 Pericarp, under D-D, which may point to subtleties in the mechanisms of breakage. But more  
571 striking than these small differences is the relative uniformity of the Mallacca compositions  
572 in relation to Outer Pericarp, Intermediate Layer and Aleurone, which vary in broadly  
573 consistent ways with particle size. This is in marked contrast to Consort, in which the  
574 relative proportions of these three components appear to vary substantially in particles of

575 different size, pointing to very different breakage origins. It appears that in the hard wheat,  
576 essentially the bran layers break “together”, with subsequent minor variations in composition  
577 as bits are knocked off. This is consistent with the general understanding that in hard wheats,  
578 the bran “breaks together with the endosperm” (Fang and Campbell, 2002a,b, 2003a), with  
579 the breakage patterns being dominated by the endosperm physical properties. By contrast, in  
580 the soft wheat, which naturally produces much larger bran particles (Campbell *et al.*, 2007;  
581 Greffeuille *et al.*, 2007) these large flat particles are then scraped by the rollers in ways that  
582 alter their composition profoundly, and more so under D-D than under S-S. The behaviour of  
583 these large bran particles is therefore dictated much more by the properties and structure of  
584 the bran layers than by the hardness of the endosperm.

585 Perhaps most interesting is the evidence that when a large flat bran particle produced from a  
586 soft wheat is scraped by the differential action of the rollers, the Intermediate Layer appears  
587 to crumble into smallish particles, while the Outer Pericarp, and to a lesser extent the  
588 Aleurone, manage to stay predominantly in large particles. This is evident under S-S, while  
589 under D-D, the contrast between the Outer Pericarp and Intermediate Layer is even more  
590 evident, with Aleurone tending more towards smaller particles in this case. This idea that the  
591 Intermediate Layer, which is physically located between the Outer Pericarp and Aleurone  
592 layers, appears to crumble into small particles whilst the layers either side remain more intact,  
593 has profound consequences for understanding the nature of wheat breakage and differences  
594 between the milling performances of different wheats. It may be that this crumbly  
595 Intermediate Layer is specific to this particular Consort sample, and not a general feature of  
596 soft wheats, in which case the implications are even more profound, particularly for Second  
597 Break milling which is devoted to scraping of large flat bran particles (Mateos-Salvador *et*  
598 *al.*, 2013). Variations in the breakage patterns of the Intermediate Layer could be exploited  
599 for developing wheats, or conditioning regimes, or First Break/Second Break roll gap  
600 combinations that lead to noticeably enhanced separation during Second Break milling.

601 Greffeuille *et al.* (2007) investigated the mechanical properties of the outer layers, Outer  
602 Pericarp, Aleurone and Intermediate layer, together and separately, for wheats of different  
603 hardness from near-isogenic lines. They confirmed that when these outer layers were intact  
604 as unseparated bran, they were more extensible in the soft wheats, consistent with the larger  
605 bran particles obtained from milling soft wheats. For the individual layers, they found that  
606 isolated Outer Pericarp was the least extensible layer, in agreement with earlier work by  
607 Antoine *et al.* (2003), and that Outer Pericarp from hard wheat was more extensible and less

608 rigid than from soft wheat. For hard wheats, the Aleurone was the most extensible of the  
609 component tissues, while in soft wheats, the Intermediate Layer was the most extensible  
610 tissue. However, when Aleurone and Intermediate Layer were tested together as adherent  
611 tissues, layers from hard and soft wheats had almost identical mechanical properties despite  
612 the different properties of the component tissues. Crucially, they concluded that for hard  
613 wheats, “the force exerted on aleurone and intermediate layers when the Outer Pericarp  
614 breaks may lead to rupture of the other tissues and consequently of the combined outer  
615 layers” while “For soft wheat, it appears that Outer Pericarp rupture does not lead to rupture  
616 of the other two tissues”. This is consistent with the current work that found that Outer  
617 Pericarp, Aleurone and Intermediate Layer tended to break together in the hard wheat but  
618 very differently in the soft wheat. Greffeuille *et al.* (2007) highlighted differences in  
619 adhesion between layers, as well as the inherent mechanical properties of each layer, as  
620 influencing the transmission of stresses between layers and their relative rupture patterns.

621 In general these results and related work (Peyron *et al.*, 2002; Antoine *et al.*, 2003;  
622 Greffeuille *et al.*, 2006) show that the mechanical properties of bran layers in hard and soft  
623 wheats vary in ways that support and help to explain the conclusion here: that bran layers  
624 tend to break together into particles of relatively uniform composition in hard wheats, while  
625 in soft wheats the bran breaks into particles that vary in their proportions of the component  
626 layers, because the component layers rupture more independently. Peyron *et al.* (2002)  
627 identify understanding of adhesion forces, structural irregularities and mechanical properties  
628 of wheat outer layers as a priority area for research into understanding wheat milling  
629 behaviour and informing wheat variety selection. The current work complements these  
630 previous studies and serves this latter goal by giving a process engineering basis for  
631 quantifying the breakage patterns of wheat tissues during milling.

632 Throughout this discussion we have been careful to highlight limitations in the scope and  
633 accuracy of the study, and clearly these tentative suggestions would be more conclusive if  
634 based on a wider range of wheats and roll gaps (if the scraping of large flat bran particles has  
635 such profound effects on bran particle composition, it would have been interesting to  
636 complement these results with those from a smaller roll gap, for which scraping would be  
637 expected to be more severe). Nevertheless, the observed patterns are sufficiently similar in  
638 certain respects and sufficient different in others, in ways that are consistent with the known  
639 effects of wheat hardness and disposition on breakage (Fang and Campbell, 2002a,b, 2003a;  
640 Campbell *et al.*, 2007) and with the understanding of the mechanical properties of bran layers

641 (Greffeuille et al., 2007), that there can be confidence that the new insights are at least  
 642 plausible. A greater understanding of the subtle effects of the physical properties of bran and  
 643 endosperm and their interaction with roll gap and disposition has the potential to lead to more  
 644 effective wheat breeding and flour milling, including the current interest in bran fractionation  
 645 to develop products enriched in certain components (Hemery et al., 2007). Meanwhile, this  
 646 work has demonstrated the new insights and quantitative understanding that can be accessed  
 647 through the compositional breakage equation approach.

648 Figure 13 shows the distributions of all four tissues (Outer Pericarp, Intermediate Layer,  
 649 Aleurone and Starchy Endosperm) plotted together on the same graph, for both wheats under  
 650 both dispositions. In this graph the distributions have been multiplied by the proportions of  
 651 each component, such that Figure 13 is the equivalent of Figure 1. The distributions  
 652 therefore add up to give the overall particle size distribution,  $\rho_2(x)$ , *i.e.* the figure is the  
 653 graphical representation of Equation 12, the compositional breakage equation in its non-  
 654 cumulative form.

655 Figure 13(a) and (c) shows dashed lines for the Mallacca and Consort wheats milled under S-  
 656 S disposition, as examples of particles of different composition. To illustrate how  
 657 compositions can be calculated, for the Mallacca wheat milled under S-S disposition, the  
 658 values of the Outer Pericarp, Intermediate Layer, Aleurone and Starchy Endosperm for  
 659 particles of size 500  $\mu\text{m}$  (shown by the dashed line in Figure 13(a)) are:

$$\begin{aligned} X_{pe}\rho_{pe}(500) &= 0.0034 & X_{in}\rho_{in}(500) &= 0.0010 \\ X_{al}\rho_{al}(500) &= 0.0032 & X_{en}\rho_{en}(500) &= 0.0707 \\ \rho_2(500) &= 0.0034+0.0010+0.0032+0.0707 & &= 0.0783 \end{aligned}$$

661 From these values, the composition of particles of 500  $\mu\text{m}$  can be calculated:

$$\begin{aligned} y_{pe}(500) &= 0.0034/0.0783 & &= 0.0434 \\ y_{in}(500) &= 0.0010/0.0783 & &= 0.0128 \\ y_{al}(500) &= 0.0032/0.0783 & &= 0.0409 \\ y_{en}(500) &= 0.0707/0.0783 & &= 0.9029 \end{aligned}$$

663 *i.e.* these particles are 4.3% Outer Pericarp, 1.3% Intermediate Layer, 4.1% Aleurone and  
 664 90.3% Starchy Endosperm.



665 Similarly, using a contrasting example, for the Consort wheat milled under S-S disposition,  
 666 the values of the Outer Pericarp, Intermediate Layer, Aleurone and Starchy endosperm for  
 667 particles of size 1500  $\mu\text{m}$  (shown by the dashed line in Figure 13(c)) are:

$$X_{pe}\rho_{pe}(1500) = 0.0078 \quad X_{in}\rho_{in}(1500) = 0.0012$$

$$668 \quad X_{al}\rho_{al}(1500) = 0.0099 \quad X_{en}\rho_{en}(1500) = 0.0721$$

$$\rho_2(1500) = 0.0078 + 0.0012 + 0.0099 + 0.0721 = 0.0910$$

669 hence

$$y_{pe}(1500) = 0.0078/0.0910 = 0.0857$$

$$670 \quad y_{in}(1500) = 0.0012/0.0910 = 0.0132$$

$$y_{al}(1500) = 0.0099/0.0910 = 0.1088$$

$$y_{en}(1500) = 0.0721/0.0910 = 0.7923$$

671 leading to a composition for these particles of 8.6% Outer Pericarp, 1.3% Intermediate Layer,  
 672 11% Aleurone and 79.2% Starchy Endosperm, i.e. these particles are much richer in bran  
 673 material and depleted in endosperm, compared with the previous example.

674 The approach presented here, allowing the particle size distribution and the component  
 675 distributions to be described by Double Kumaraswamy Functions, the ratios of which give  
 676 the concentration functions, is a practical way to describe, quantify and interpret the effects of  
 677 breakage on component distributions. This approach also represents the continuous  
 678 equivalent of the discrete compositional breakage matrices introduced by Fistes and Tanovic  
 679 (2006), yielding greater predictive power and greater mechanistic insights in wheat breakage.  
 680 More work is needed to evaluate the accuracy of the spectroscopic predictions for this sort of  
 681 application, and to apply the approach to a wider range of milled samples in order to lead to  
 682 more confident conceptions of the physical breakage mechanisms operating during roller  
 683 milling of wheat and the compositional and structural factors influencing these.

684

## 685 **Conclusions**

686 The distributions of wheat kernel components within eight size fractions of Mallacca and  
 687 Consort wheats milled under S-S and D-D dispositions have been quantified by PLS models  
 688 developed by Barron (2011), and the concentration functions found by fitting Double

689 Normalised Kumaraswamy Breakage Functions to the particle size distribution and to the  
690 compositional distributions. The DNKBF was found to describe the data well for the four  
691 botanical components studied: Outer Pericarp, Intermediate Layer, Aleurone and Starchy  
692 Endosperm, for both wheat types and both dispositions. For the hard Mallacca wheat, the  
693 Outer Pericarp and Aleurone layer compositions mostly varied with particle size in similar  
694 ways, consistent with these layers fusing together as “bran” and breaking together, although  
695 with possibly a subtle difference around the production of very fine particles under D-D  
696 milling. Although the data calculated for the Intermediate Layer by the spectroscopic model  
697 was less accurate compared with the other botanical tissues, the results show a broadly  
698 similar pattern to those for Outer Pericarp and Aleurone in the Mallacca wheat, adding  
699 confidence that the features observed are genuine. However, for Consort wheat, the  
700 Intermediate Layer behaved differently from Outer Pericarp and Aleurone, suggesting a  
701 different breakage mechanism which could be associated with how wheat hardness affects  
702 breakage of the bran and the production of large flat bran particles. This finding gives new  
703 insights into the nature of wheat breakage, and the contribution of the Intermediate Layer  
704 tissues to breakage, that could have implications for wheat breeding and flour mill operation  
705 as well as bran fractionation processes to recover nutritionally enhanced fractions.

706 The data from both wheats under the two milling dispositions highlighted consistent patterns  
707 and some distinctive differences that together give a degree of confidence that the apparent  
708 effects are genuine. The contrast between the hard Mallacca wheat and the soft Consort  
709 wheat is more evident than the difference between the S-S and D-D dispositions. Some  
710 interesting patterns within the compositional data for Mallacca are observed, like the  
711 Aleurone peak being shifted to the right compared with the Outer Pericarp peak, which is also  
712 evident for Consort under S-S, and the apparent production of Outer Pericarp/Intermediate  
713 Layer/Aleurone dust under S-S, but only Intermediate Layer/Aleurone dust, without Outer  
714 Pericarp, under D-D, which may point to subtleties in the mechanisms of breakage. The  
715 relative uniformity of the Mallacca compositions in relation to Outer Pericarp, Intermediate  
716 Layer and Aleurone, which vary in roughly consistent ways with particle size, is notable.  
717 This is in contrast to Consort, in which the relative proportions of these three components  
718 appear to vary substantially in particles of different size, pointing to very different breakage  
719 origins.

720 It is suggested tentatively that in the hard wheat the bran layers break “together”, with  
721 subsequent minor variations in composition as bits are knocked off. By contrast, in the soft

722 wheat, which naturally produces much larger bran particles, these large flat particles are then  
723 scraped in such a way that their composition changes profoundly, and more so under D-D  
724 than under S-S. The behaviour of these large bran particles is therefore dictated more by the  
725 properties and structure of the bran layers than by the hardness of the endosperm. The  
726 current work complements previous studies of the mechanical properties of bran layers by  
727 giving a quantitative process engineering basis for understanding wheat breakage  
728 mechanisms in order to inform milling practice and wheat breeding.

729

### 730 **Acknowledgements**

731 SPGN gratefully acknowledges the National Council of Science and Technology of Mexico  
732 (CONACyT), the Mexican Government and the Ministry of Public Education (SEP) for  
733 financial support to undertake this work. The Satake Corporation of Japan is gratefully  
734 acknowledged for its support in establishing the activities of the Satake Centre for Grain  
735 Process Engineering.

736

737

### 738 **References**

- 739 Antoine, C., Peyron, S., Mabilhe, F., Lapierre, C., Bouchet, B., Abecassis, J. and Rouau X.  
740 2003. Individual contribution of grain outer layers and their cell wall structure to the  
741 mechanical properties of wheat bran. *J Agric Food Chem* 51:2026–2033.
- 742 Barron, C. 2011. Prediction of relative tissue proportions in wheat mill streams by Fourier  
743 Transform Mid-infrared spectroscopy. *J Agric Food Chem.* 59: 10442–10447.
- 744 Barron, C. and Rouau, X. 2008. FTIR and Raman signatures of wheat grain peripheral  
745 tissues. *Cereal Chem.* 85:619-625.
- 746 Barron, C., Surget, A. and Rouau, X. 2007. Relative amounts of tissues in mature wheat  
747 (*Triticum aestivum* L.) grain and their carbohydrate and phenolic acid composition. *J*  
748 *Cereal Sci*, 45:88-96.
- 749 Barron, C., Samson, M.-F., Lullien-Pellerin, V. and Rouau, X. 2011. Wheat grain tissue  
750 proportions in milling fractions using biochemical marker measurements: Application  
751 to different wheat cultivars. *J Cereal Sci.* 53:306-311.
- 752 Broadbent, S. R. and Callcott, T. G. 1956a. Coal breakage processes. I. A new analysis of  
753 coal breakage processes. *J Inst Fuel* 29:524-528.
- 754 Broadbent, S. R. and Callcott, T. G. 1956b. Coal breakage processes. II. A matrix  
755 representation of breakage. *J Inst Fuel* 29:528-539.
- 756 Broadbent, S. R. and Callcott, T. G. 1957. Coal breakage processes. IV. An exploratory  
757 analysis of the cone mill in open circuit grinding. *J Inst Fuel* 30:18-21.
- 758 Campbell, G. M. and Webb, C. 2001. On predicting roller milling performance I: The  
759 breakage equation. *Powder Technol.* 115:234-242.
- 760 Campbell, G. M., Bunn, P. J., Webb, C. and Hooks, S. C. W. 2001. On predicting roller  
761 milling performance II: The breakage function. *Powder Technol.* 115:243:255.

- 762 Campbell, G. M., Fang, C. and Muhamad, I. I. 2007. On predicting roller milling  
763 performance VI: Effect of kernel hardness and shape on the particle size distribution  
764 from first break milling of wheat. *Food Bioprod Process.* 85:7-23.
- 765 Campbell, G. M., Sharp, C., Wall, K., Mateos-Salvador, F., Gubatz, S., Huttly, A. and  
766 Shewry, P. 2012. Modelling wheat breakage during roller milling using the Double  
767 Normalised Kumaraswamy Breakage function: Effects on kernel shape and hardness.  
768 *J Cereal Sci.* 55:415-425.
- 769 Choomjaihan, P. 2009. Extending the breakage equation on first break milling of wheat to  
770 include particle composition. PhD thesis. The University of Manchester, UK.
- 771 Fang, C. and Campbell, G. M. 2002a. Effect of roll fluting disposition and roll gap on  
772 breakage of wheat kernels during first break roller milling. *Cereal Chem* 79:518-522.
- 773 Fang, C. and Campbell, G. M. 2002b. Stress-strain analysis and visual observation of wheat  
774 kernel breakage during roller milling using fluted rolls. *Cereal Chem* 79:511-517.
- 775 Fang, C. and Campbell, G. M. 2003a. On predicting roller milling performance IV: Effect of  
776 roll disposition on the particle size distribution from first break milling of wheat. *J*  
777 *Cereal Sci* 37:21-29.
- 778 Fang, C. and Campbell, G. M. 2003b. On predicting roller milling performance V: Effect of  
779 moisture content on the particle size distribution from first break milling of wheat. *J*  
780 *Cereal Sci* 37: 31-41.
- 781 Fistes, A. and Tanovic, G. 2006. Predicting the size and compositional distributions of wheat  
782 flour stocks following first break roller milling using the breakage matrix approach. *J*  
783 *Food Eng* 75:527-534.
- 784 Fuh, K. F., Coate, J. M. and Campbell, G. M. 2014. Effects of roll gap, kernel shape and  
785 moisture on wheat breakage modelled using the Double Normalised Kumaraswamy  
786 Breakage Function. *Cereal Chem* 91:8-17.
- 787 Galindez-Najera, S. P. and Campbell, G. M. 2014. Modelling first break milling of debranned  
788 wheat using the Double Normalised Kumaraswamy Breakage function. *Cereal Chem*  
789 91, 533-541.
- 790 Galindez-Najera, S. P. 2014. A compositional breakage equation for first break roller milling  
791 of wheat. PhD thesis. The University of Manchester, UK.
- 792 Greffeuille, V., Abecassis, J., Lapierre C. and Lullien-Pellerin, V. 2006. Bran Size  
793 Distribution at Milling and Mechanical and Biochemical Characterization of Common  
794 Wheat Grain Outer Layers: A Relationship Assessment. *Cereal Chem* 83:641-646.
- 795 Greffeuille, V., Mabile, F., Rousset, M., Oury, F.-X., Abecassis, J., Lullien-Pellerin, V.  
796 2007. Mechanical properties of outer layers from near-isogenic lines of common wheat  
797 differing in hardness. *J Cereal Sci* 45, 227–235.
- 798 Hemery, Y., Rouau, X., Lullien-Pellerin, V., Barron, C. and Abecassis, J. 2007. Dry  
799 processes to develop wheat fractions and products with enhanced nutritional quality. *J*  
800 *Cereal Sci* 46:327-347.
- 801 Hemery, Y., Lullien-Pellerin, V., Rouau, X., Abecassis, J., Samson M-F., Aman, P., von  
802 Reding, W., Spoerndli, C. and Barron, C. 2009. Biochemical markers: Efficient tools  
803 for the assessment of wheat grain tissue proportions in milling fractions *J Cereal Sci*  
804 49:55-64.
- 805 Mateos-Salvador, F., Sadhukhan, J. and Campbell, G. M., 2013. Extending the Normalised  
806 Kumaraswamy Breakage function of roller milling of wheat flour stocks to Second  
807 break. *Powder Technol* 237:107-116.

- 808 Peyron, S., Surget, A., Mabile, F., Autran, J.C., Rouau, X. and Abecassis, J. 2002.  
809 Evaluation of tissue dissociation of durum wheat grain (*Triticum durum* Desf.)  
810 generated by the milling process. *J Cereal Sci* 36:199-208.  
811 Pomeranz, Y. 1988. Wheat Chemistry and Technology II, 3<sup>rd</sup> Edition. American Association  
812 of Cereal Chemists. St Paul, MN, USA, pp285-328.

ACCEPTED MANUSCRIPT

Table 1. Particle size distributions and compositions of size fractions following milling of Mallacca and Consort wheats under Sharp-to-Sharp and Dull-to-Dull dispositions.

Sieve Size (µm)	Percentage on sieve	Pericarp concentration (%)	Intermediate Layer concentration (%)	Aleurone concentration (%)	Starchy Endosperm concentration (%)
Mallacca					
Sharp-to-Sharp					
2000	7.92	12.6	5.5	6.6	75.4
1700	10.78	11.4	2.0	11.4	75.3
1400	19.49	11.7	1.6	6.1	80.6
1180	12.87	13.9	2.4	8.9	74.8
850	14.88	12.7	1.1	5.5	80.7
500	14.09	6.5	2.0	2.4	89.2
212	10.88	3.9	0.7	7.0	88.4
0	9.10	9.2	1.9	9.7	79.2
Average		10.4	2.0	6.9	80.8
Dull-to-Dull					
2000	35.74	8.9	3.6	5.2	82.3
1700	11.66	15.2	3.0	7.1	74.7
1400	10.35	14.2	0.9	8.5	76.4
1180	5.14	13.3	2.7	3.6	80.4
850	6.47	8.9	2.5	2.1	86.4
500	10.75	5.7	1.7	5.1	87.5
212	11.06	7.8	0.0	4.5	87.7
0	8.83	2.1	4.1	7.3	86.5
Average		9.3	2.6	5.6	82.5
Whole grain		8.3	1.2	6.0	84.4
Consort					
Sharp-to-Sharp					
2000	17.93	3.8	3.5	11.0	81.8
1700	10.35	5.6	2.3	13.0	79.1
1400	14.37	7.2	2.8	11.7	78.3
1180	10.39	9.8	0.0	8.2	82.0
850	9.94	7.3	1.7	7.4	83.6
500	15.0	3.6	3.0	6.5	86.9
212	11.79	0.1	3.1	4.0	92.8
0	10.23	0.9	3.8	2.8	92.5
Average		4.7	2.6	8.3	84.4
Dull-to-Dull					
2000	37.95	6.5	3.8	15.1	74.6
1700	8.86	8.3	1.4	11.8	78.5
1400	6.91	7.0	1.4	13.2	78.4
1180	4.78	9.5	1.1	12.9	76.5
850	6.31	4.7	1.9	9.1	84.3
500	12.09	0.9	4.1	5.6	89.4
212	12.16	0.0	4.5	7.0	88.6
0	10.95	0.0	3.6	10.3	86.1
Average		4.5	3.2	11.5	80.7
Whole grain		2.3	2.9	5.8	88.9

Table 2. Fitted DNKBF parameters.

	$\alpha$	$m_1$	$n_1$	$m_2$	$n_2$
<b>MALLACCA</b>					
Sharp-to-Sharp (S-S)					
PSD	0.358	5.54	178	1.08	3.44
Pericarp	0.733	4.05	53.9	0.38	0.91
Intermediate layer	0.374	4.81	100	0.79	1.26
Aleurone	0.558	5.18	100	0.63	2.13
Starchy endosperm	0.293	6.29	343	1.18	3.98
Dull-to-Dull (D-D)					
PSD	0.379	7.89	99.9	0.92	2.36
Pericarp	0.419	6.44	99.9	1.06	1.59
Intermediate layer	0.263	7.04	99.9	0.41	0.47
Aleurone	0.455	7.00	99.9	0.61	1.44
Starchy endosperm	0.395	8.16	99.9	0.97	2.91
<b>CONSORT</b>					
Sharp-to-Sharp (S-S)					
PSD	0.143	8.21	1526	0.99	2.24
Pericarp	0.790	4.02	53.9	0.75	0.63
Intermediate layer	0.421	7.24	100	1.15	7.94
Aleurone	0.356	5.65	100	1.24	2.25
Starchy endosperm	0.124	6.74	343	0.95	2.29
Dull-to-Dull (D-D)					
PSD	0.432	8.67	99.9	0.98	3.79
Pericarp	0.228	4.36	99.7	6.13	24.25
Intermediate layer	0.286	2.28	100	0.35	0.31
Aleurone	0.133	6.16	99.9	0.49	0.51
Starchy endosperm	0.421	8.56	99.9	1.03	4.93

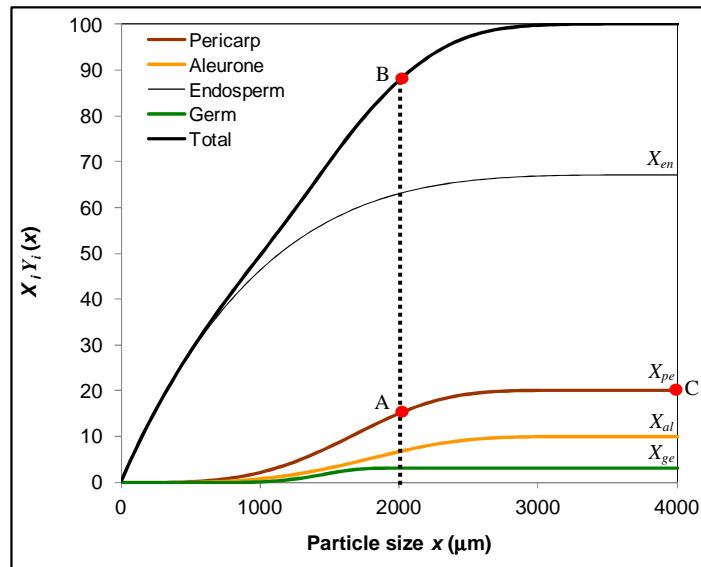


Figure 1. Contrived example that shows how the cumulative PSD is comprised of the cumulative distributions of the four botanical components in particles of different sizes. Adapted from Choomjaihan (2009).



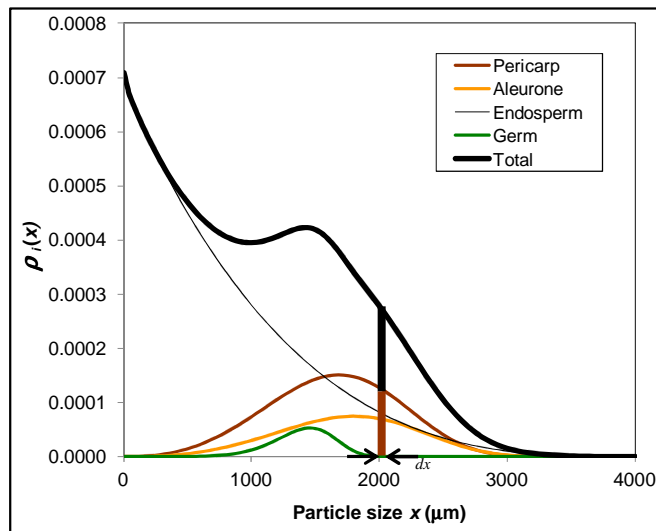


Figure 2. Non-cumulative form of the contrived example of Figure 6.1, displaying how particles of different size are made up of different compositions. Adapted from Choomjaihan (2009).

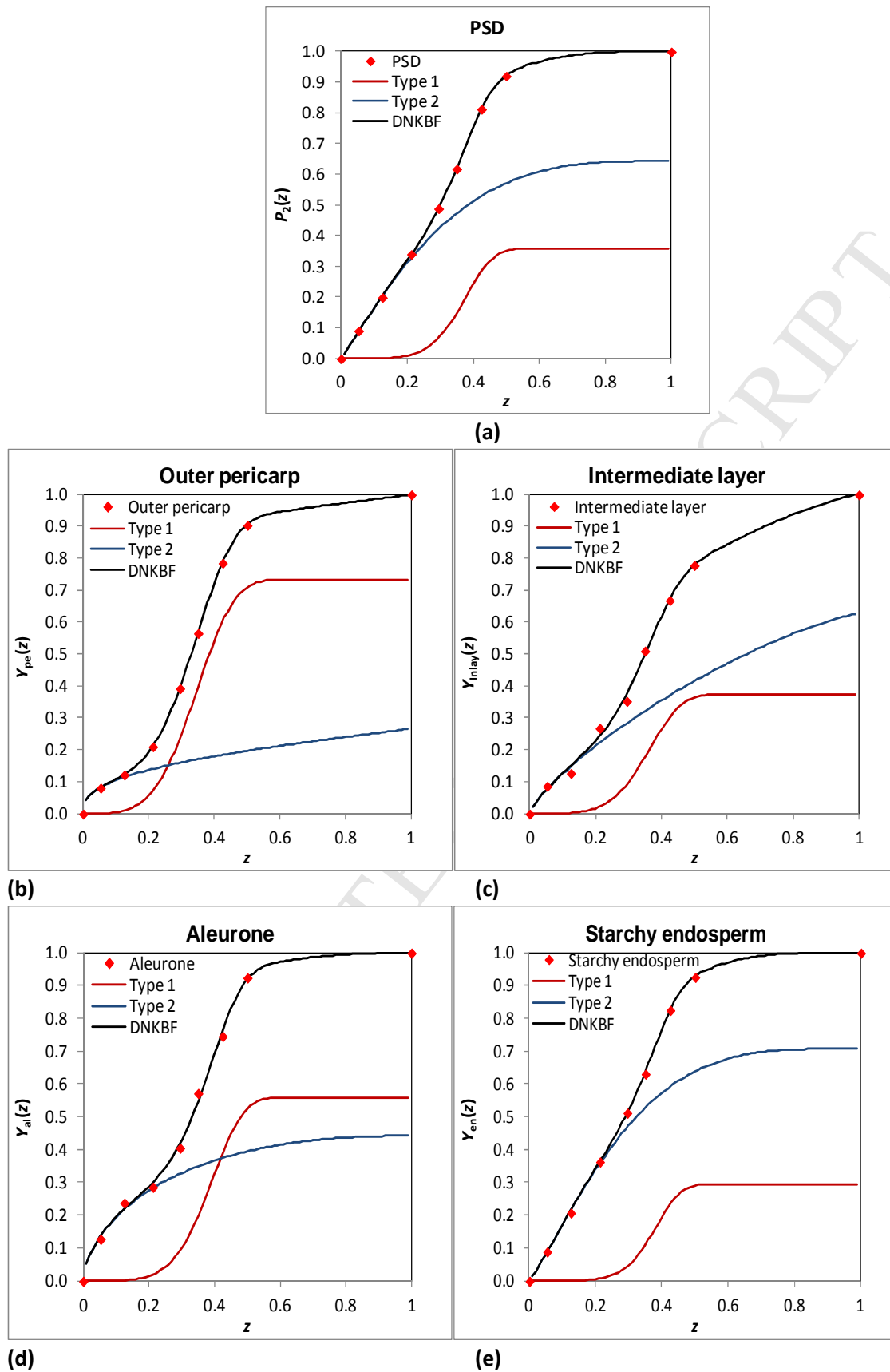


Figure 3. Cumulative particle size and component distributions, for Mallacca wheat milled under a Sharp-to-Sharp disposition.

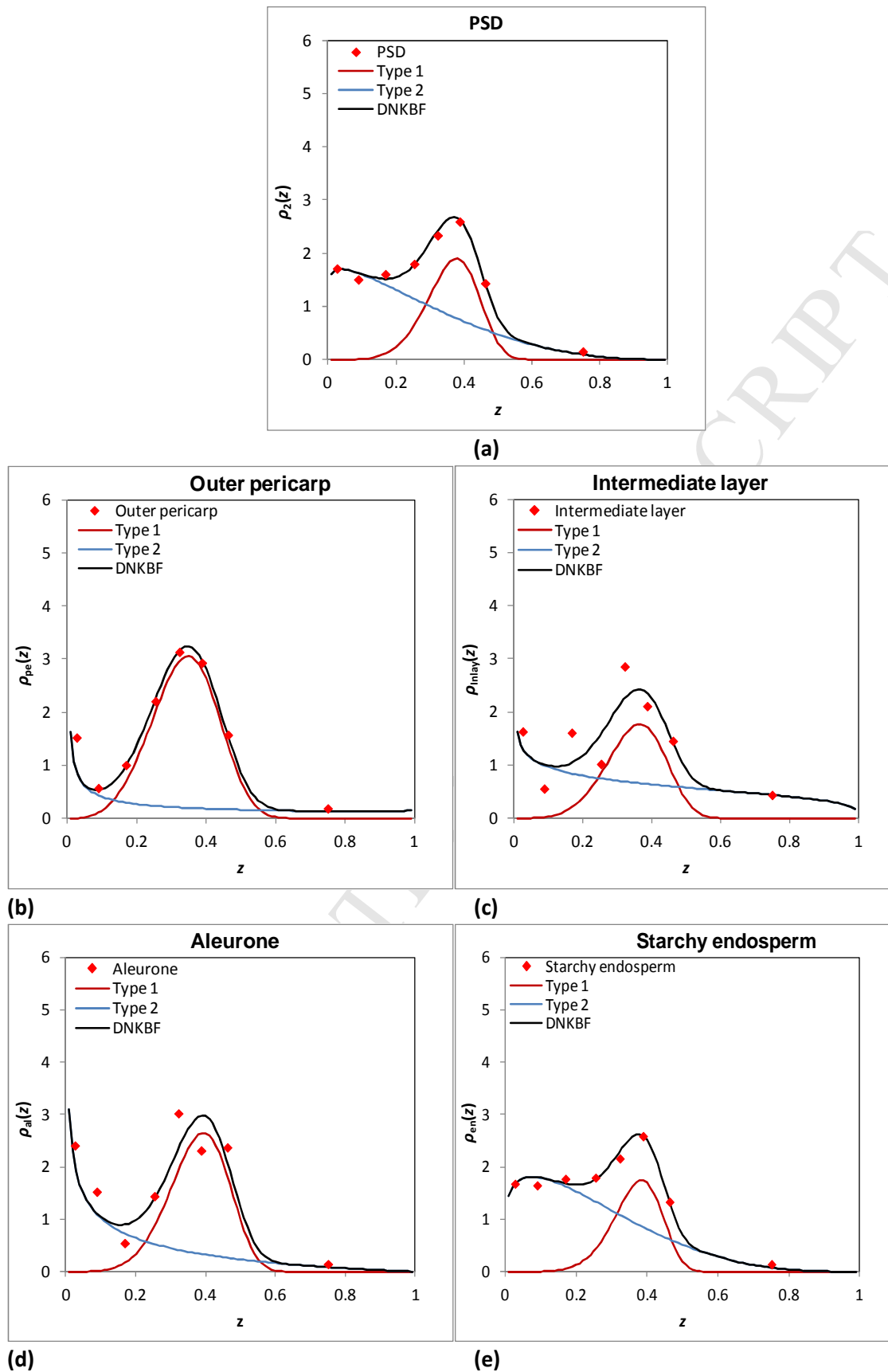


Figure 4. Non-cumulative particle size and component distributions, for Mallacca wheat milled under a Sharp-to-Sharp disposition.

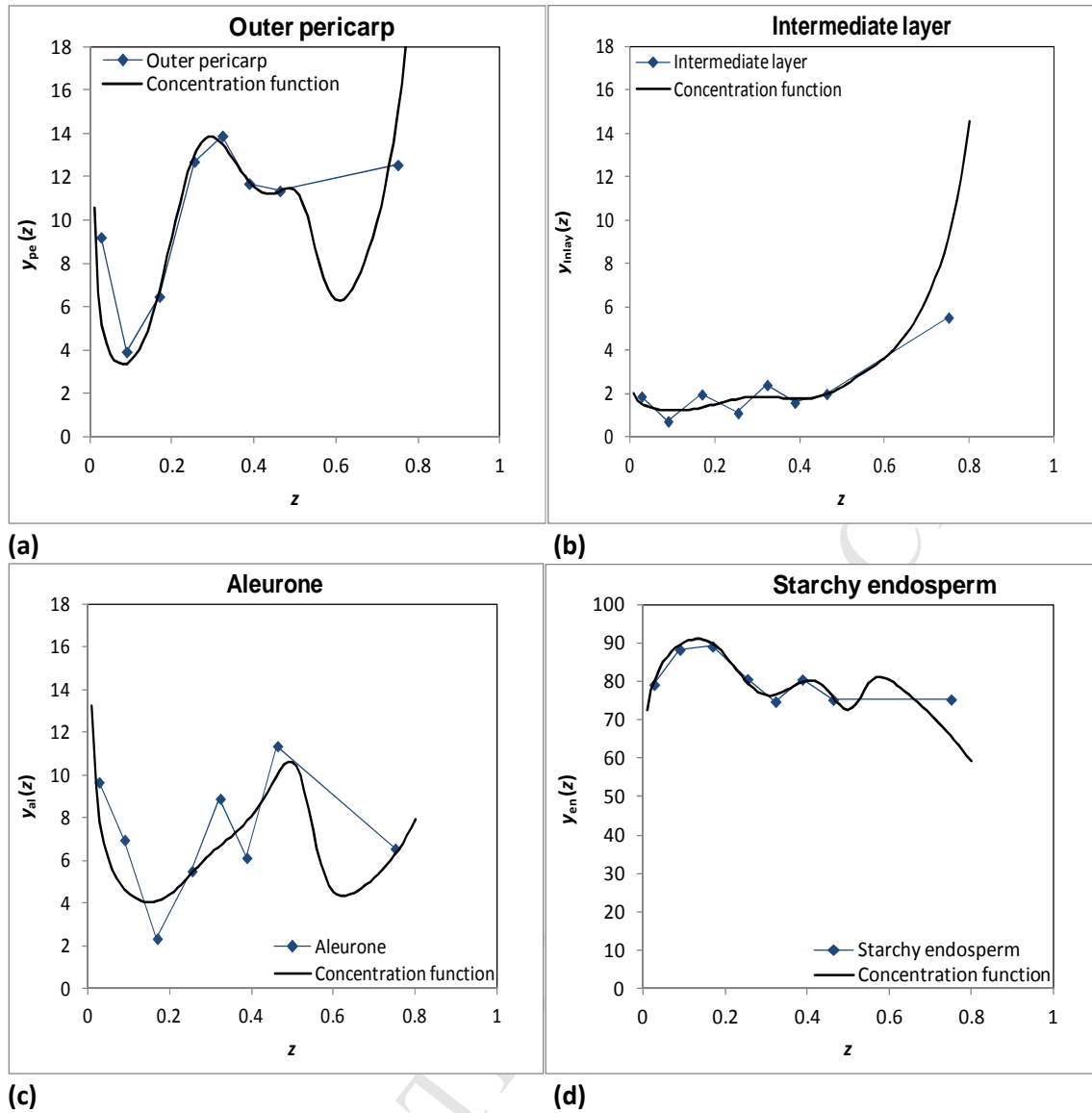
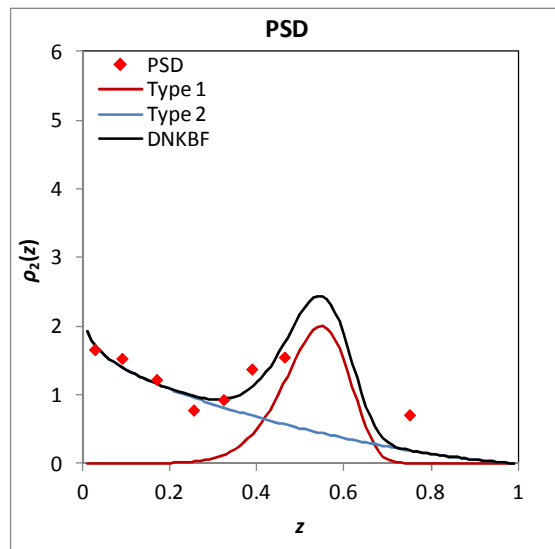
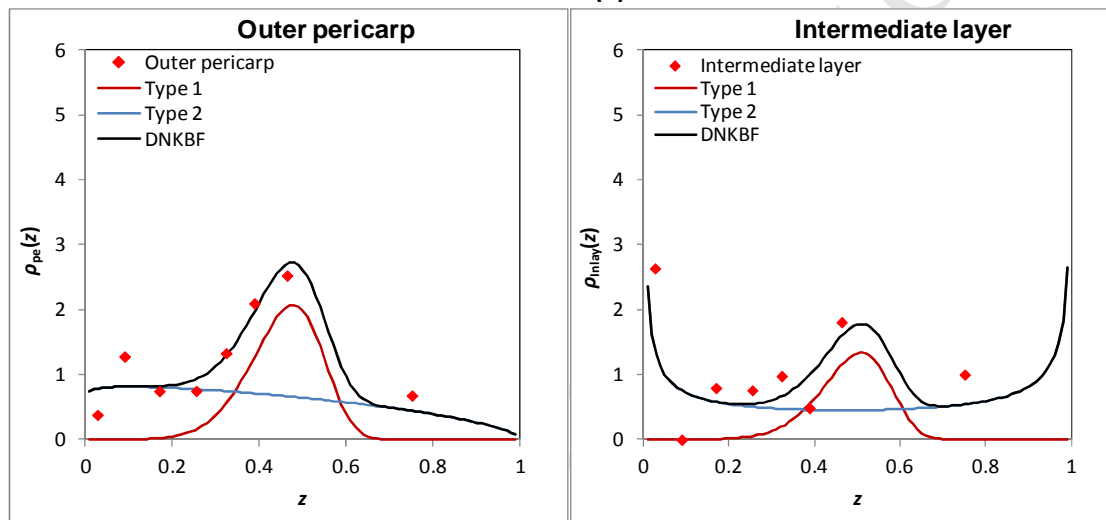


Figure 5. Concentration functions for outer pericarp, intermediate layer, aleurone and starchy endosperm, compared with experimental data, for Mallacca wheat milled under Sharp-to-Sharp disposition.

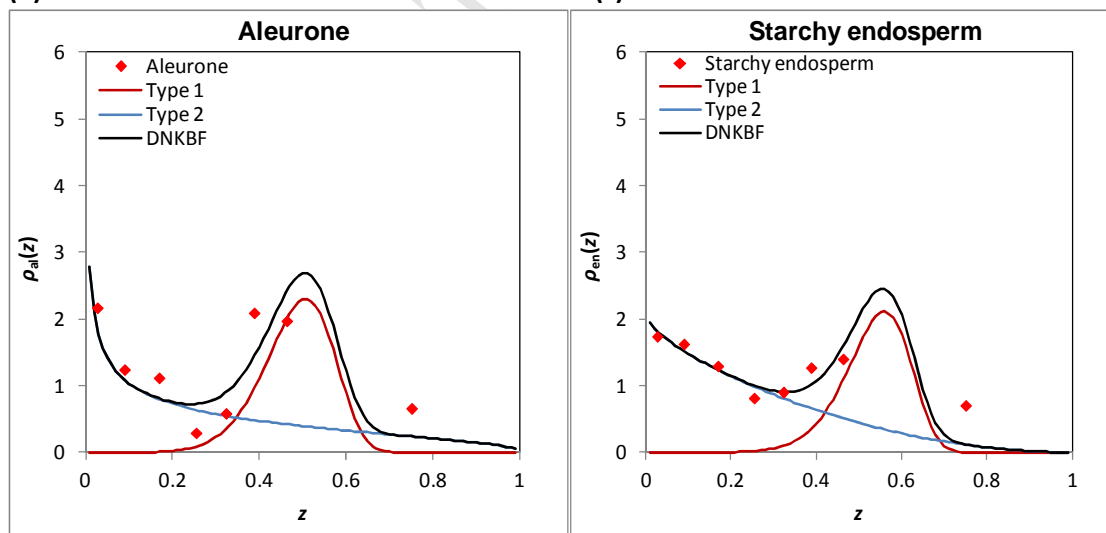


(a)



(b)

(c)



(d)

(e)

Figure 6. Non-cumulative particle size and component distributions, for Mallacca wheat milled under a Dull-to-Dull disposition.

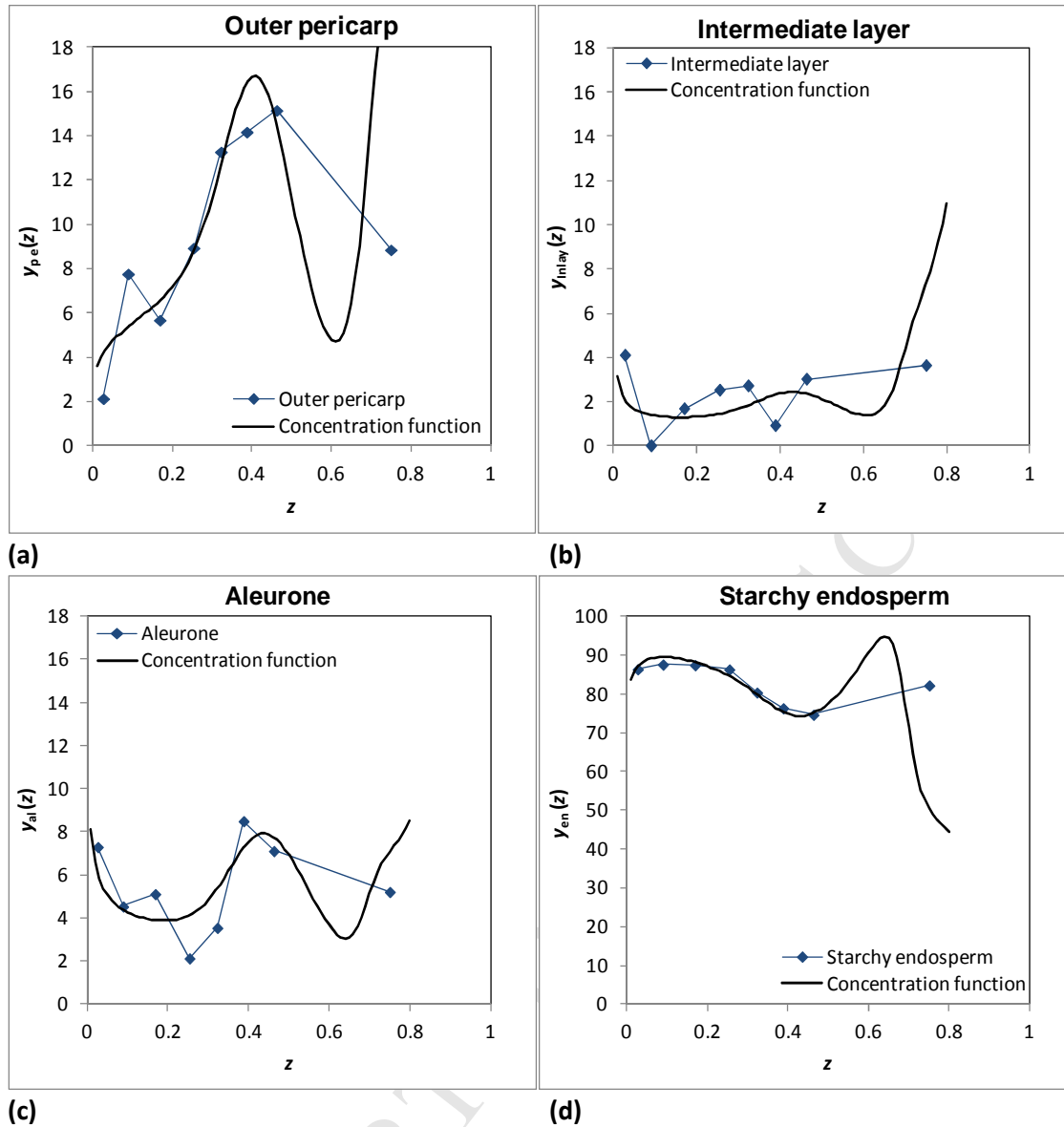
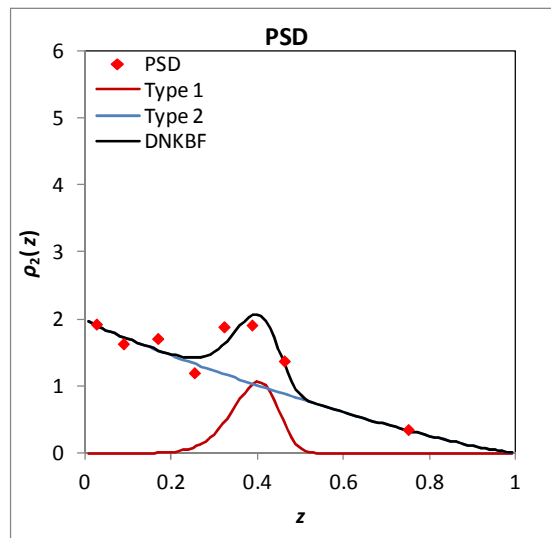
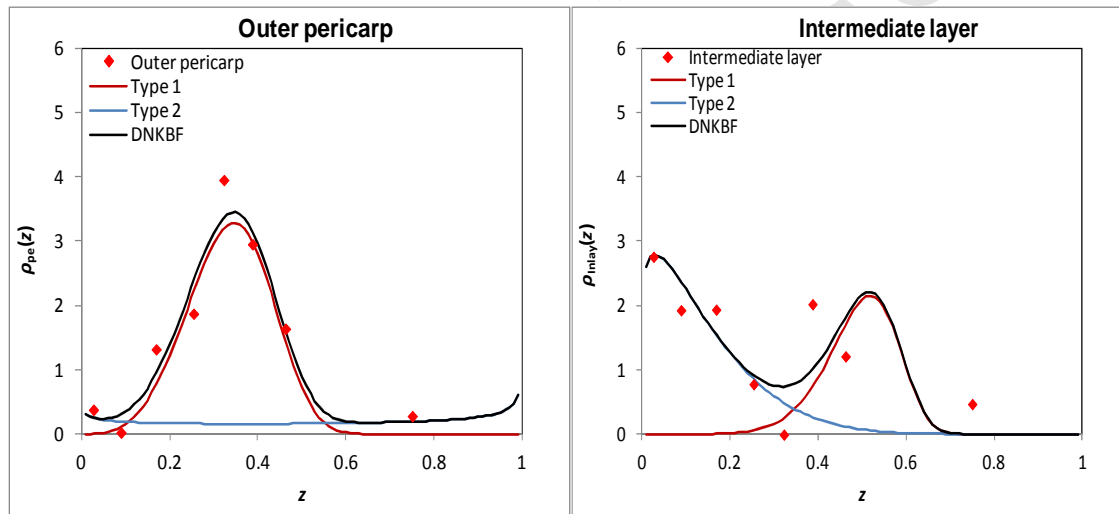


Figure 7. Concentration functions for outer pericarp, aleurone, endosperm and intermediate layer, compared with experimental data, for Mallacca wheat milled under a Dull-to-Dull disposition.

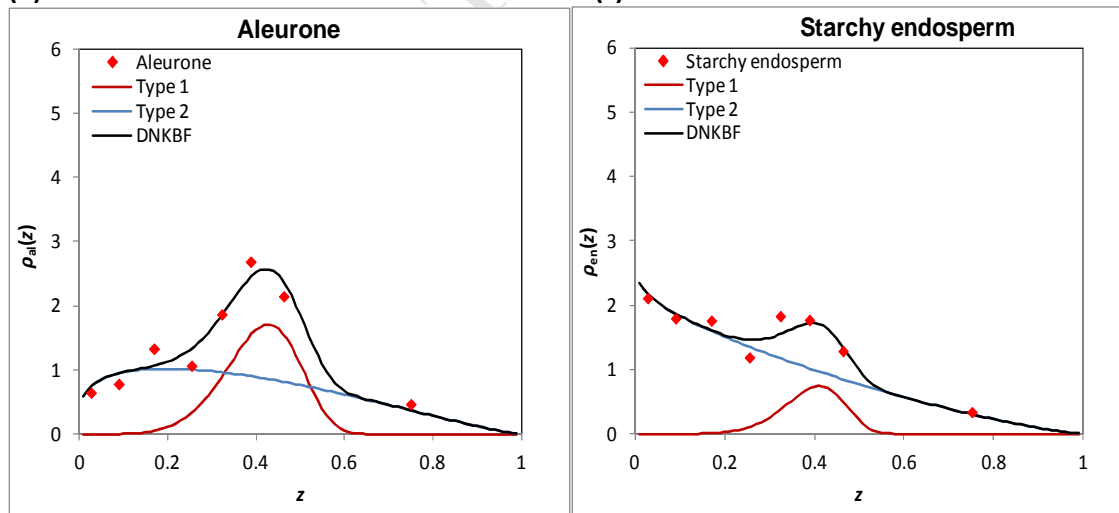


(a)



(b)

(c)



(d)

(e)

Figure 8. Non-cumulative particle size and component distributions, for Consort wheat milled under a Sharp-to-Sharp disposition.

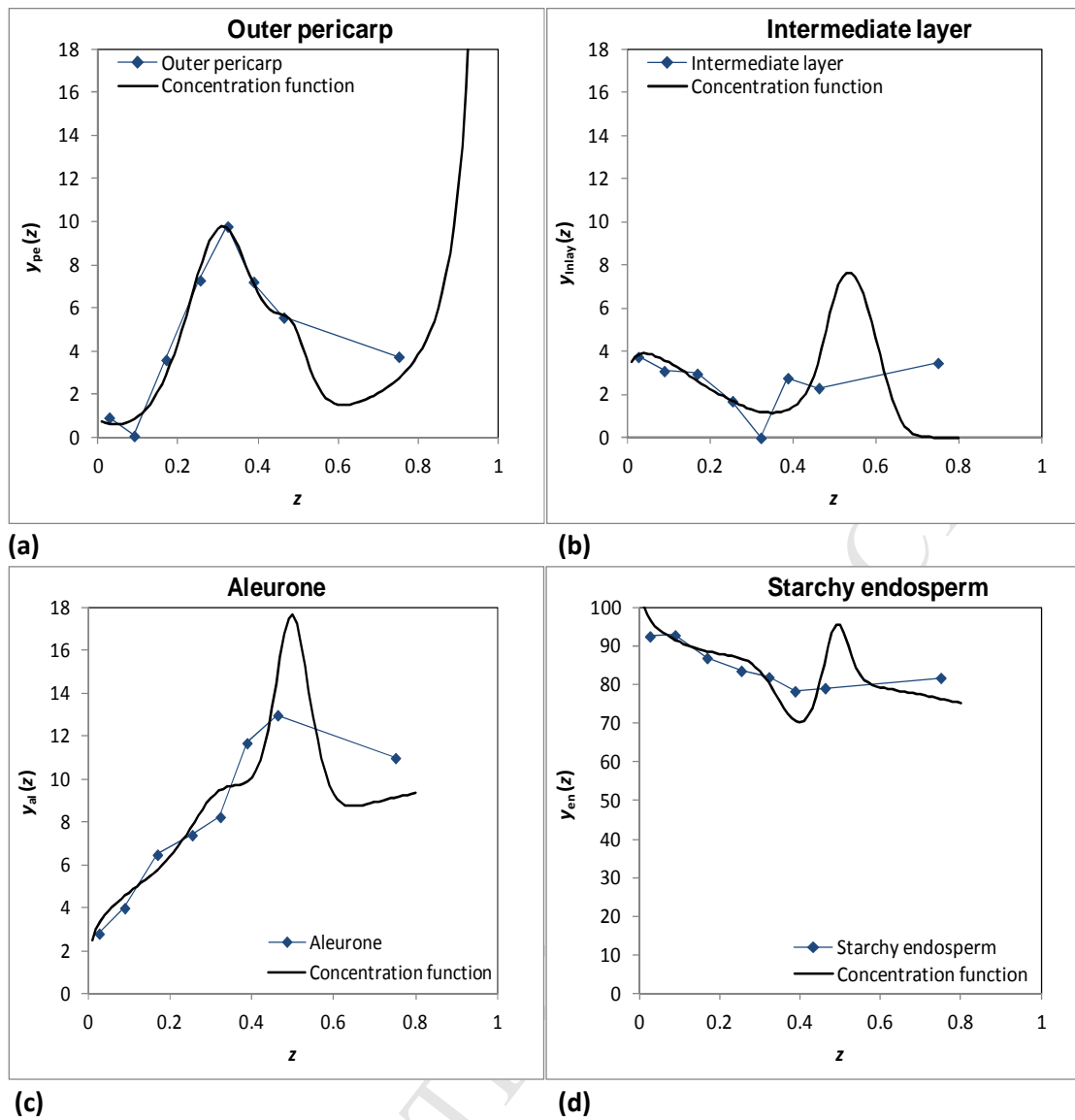
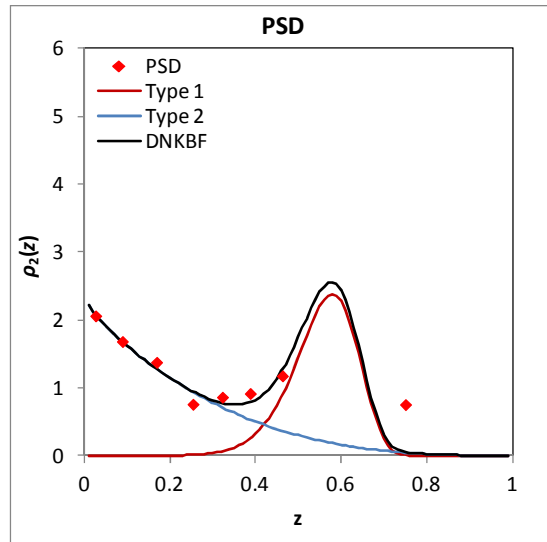
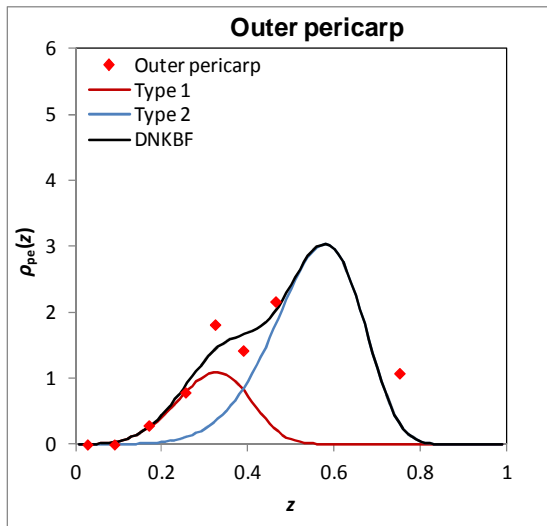


Figure 9. Concentration functions for outer pericarp, intermediate layer, aleurone and starchy endosperm, compared with experimental data, for Consort wheat milled under a Sharp-to-Sharp disposition.

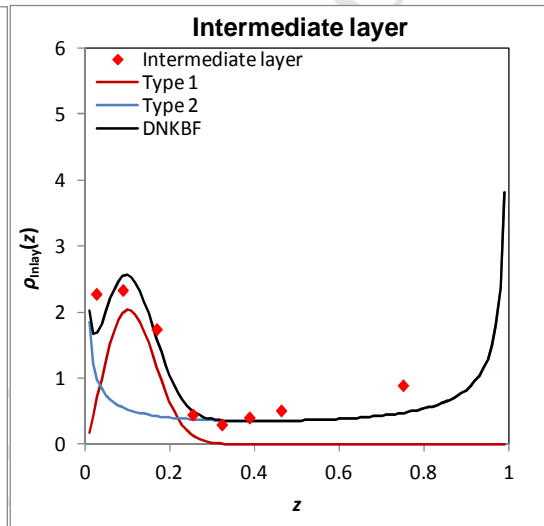




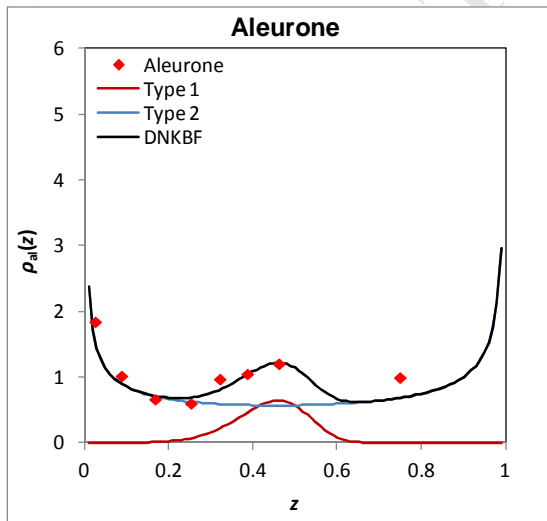
(a)



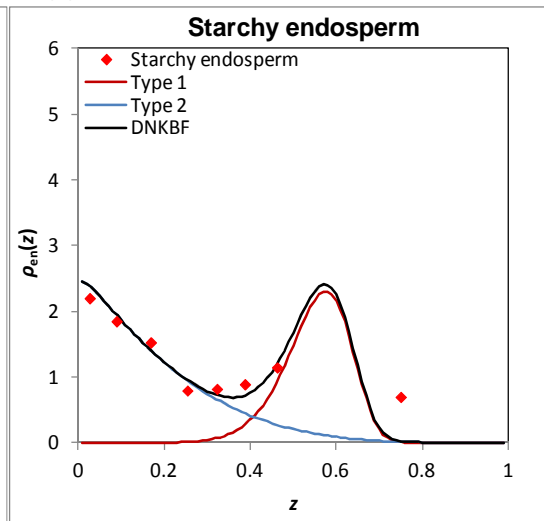
(b)



(c)



(d)



(e)

Figure 10. Non-cumulative particle size and component distributions, for Consort wheat milled under a Dull-to-Dull distribution.

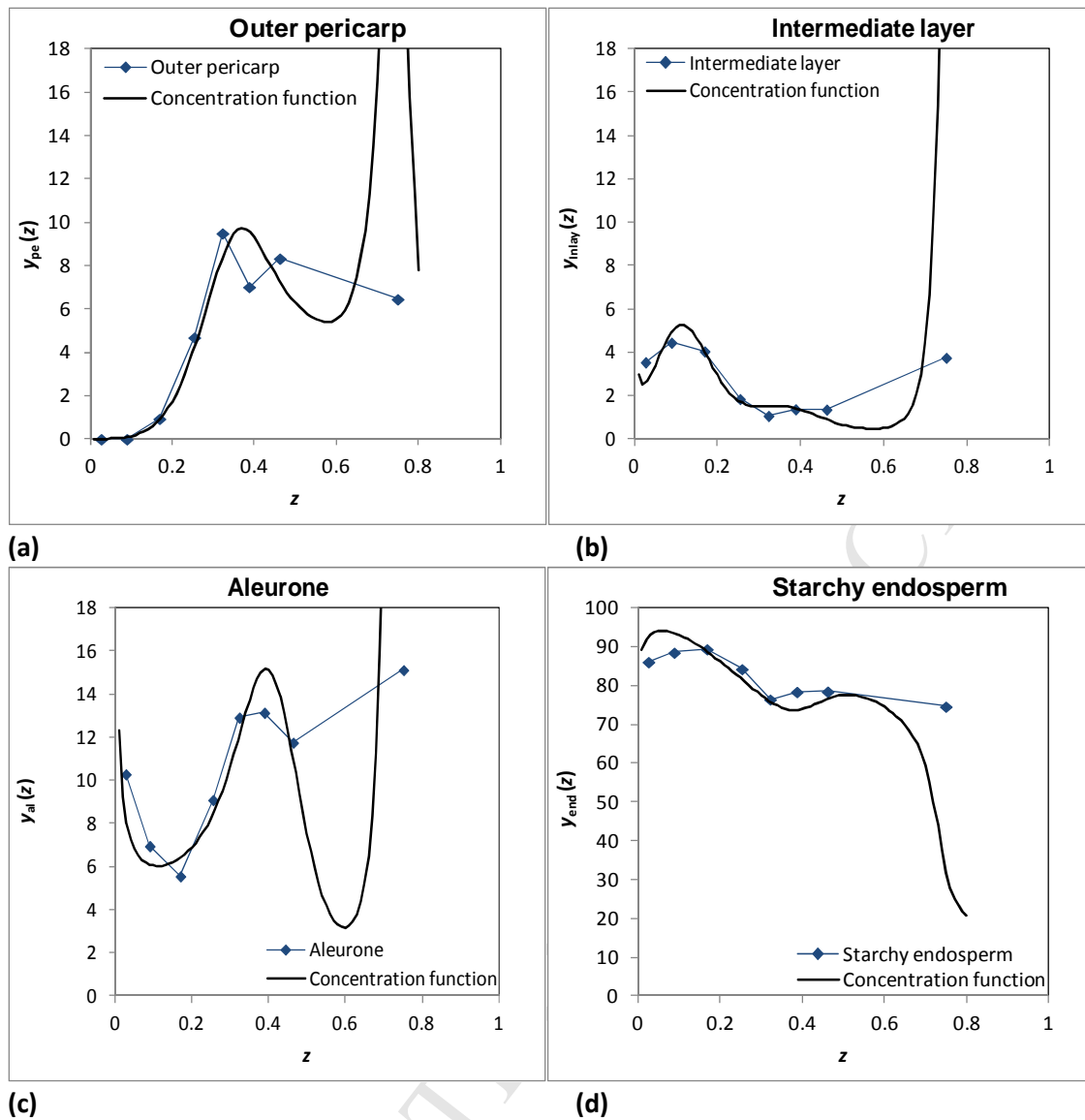


Figure 11. Concentration functions for outer pericarp, aleurone, endosperm and intermediate layer, compared with experimental data, for Consort wheat milled under a Dull-to-Dull disposition.

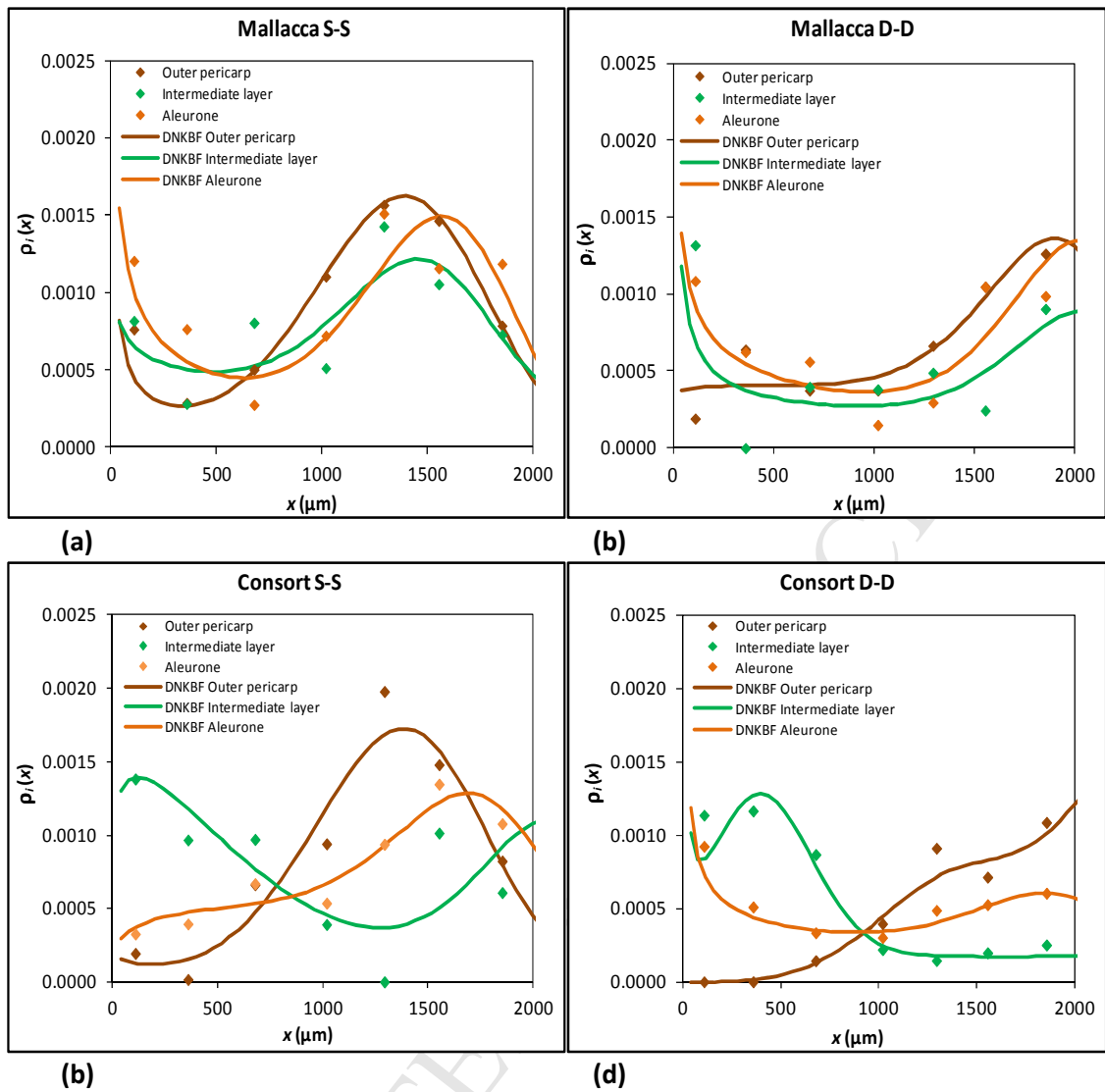


Figure 12. Outer pericarp, intermediate layer and aleurone distributions for Mallacca (a,b) and Consort (c,d) wheats milled under a Sharp-to-Sharp (a,c) and Dull-to-Dull (b,d) dispositions.

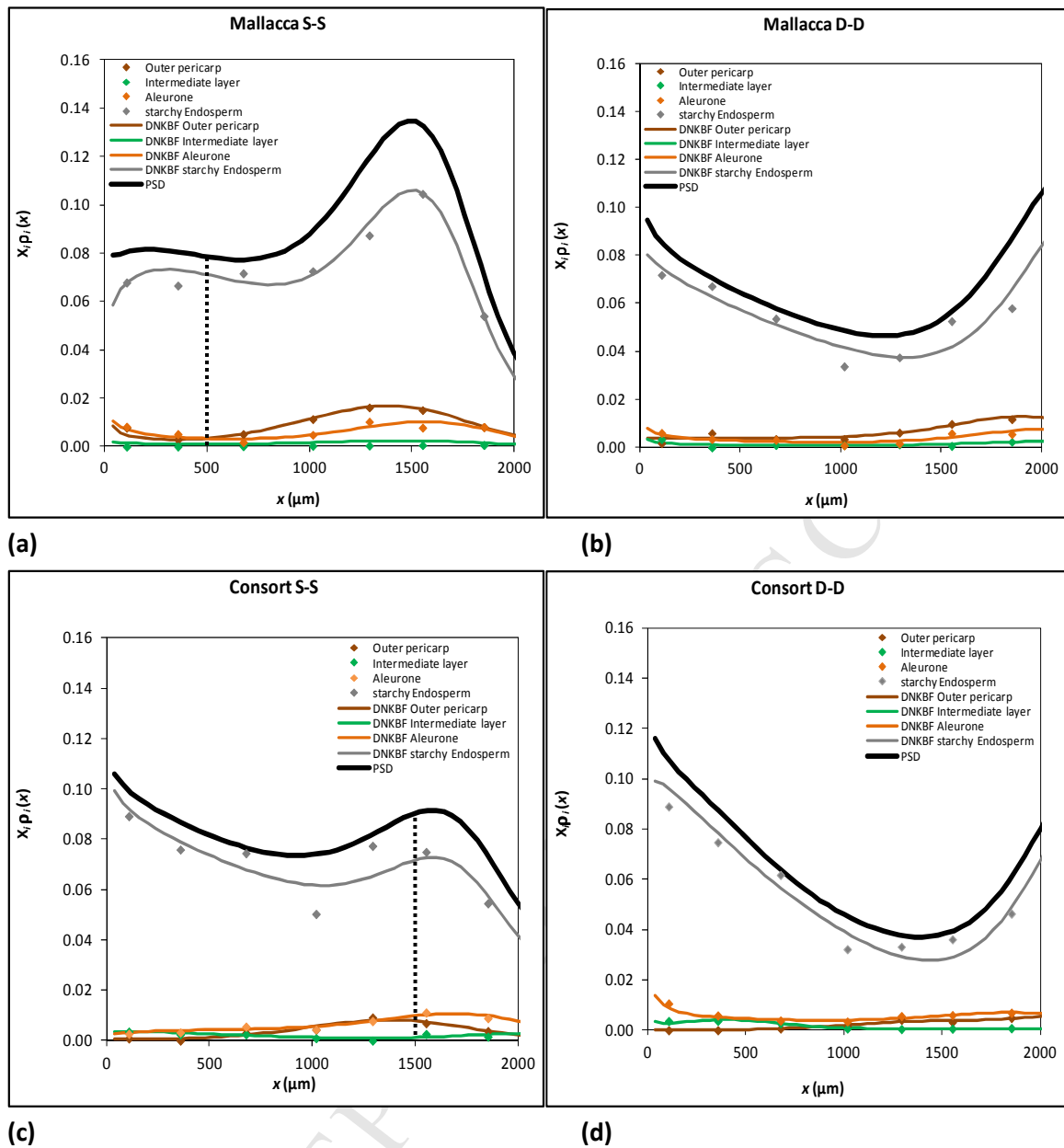


Figure 13. Outer pericarp, intermediate layer, aleurone and starchy endosperm distributions for Mallacca (a,b) and Consort (c,d) wheats milled under (a,c) Sharp-to-Sharp (a,c), and Dull-to-Dull (b,d) dispositions.

**Highlights**

The breakage equation for roller milling of wheat was extended to include composition

Compositional breakage functions were formulated based on spectroscopic models

Composition modelled in terms of Pericarp, Intermediate Layer, Aleurone and Endosperm

In a hard wheat these layers tended to break together, but separately in a soft wheat

ACCEPTED MANUSCRIPT

Comment citer ce document :

Galindez-Najera, S., Choomjaihan, P., Barron, C., Lullien-Pellerin, V., Campbell, G. (2016). A compositional breakage equation for wheat milling. *Journal of Food Engineering*, 182, 46–64.

DOI : 10.1016/j.jfoodeng.2016.03.001